

A model of chiral spin liquids with Abelian and non-Abelian topological phases

Jyong-Hao Chen,¹ Christopher Mudry,¹ Claudio Chamon,² and A. M. Tsvelik³

¹*Condensed Matter Theory Group, Paul Scherrer Institute, CH-5232 Villigen PSI, Switzerland*

²*Department of Physics, Boston University, Boston, MA, 02215, USA*

³*Condensed Matter Physics and Materials Science Division,
Brookhaven National Laboratory, Upton, NY 11973-5000, USA*

(Dated: August 23, 2017)

We present a two-dimensional lattice model for quantum spin-1/2 for which the low-energy limit is governed by four flavors of strongly interacting Majorana fermions. We study this low-energy effective theory using two alternative approaches. The first consists of a mean-field approximation. The second consists of a Random Phase approximation (RPA) for the single-particle Green's functions of the Majorana fermions built from their exact forms in a certain one-dimensional limit. The resulting phase diagram consists of two competing chiral phases, one with Abelian and the other with non-Abelian topological order, separated by a continuous phase transition. Remarkably, the Majorana fermions propagate in the two-dimensional bulk, as in the Kitaev model for a spin liquid on the honeycomb lattice. We identify the vison fields, which are mobile (they are static in the Kitaev model) domain walls propagating along only one of the two space directions.

CONTENTS

I. Introduction and results	1
A. Motivation	1
B. Results and outline	3
II. Majorana field theory	4
A. Definition	4
B. Limiting cases	5
III. Mean-field approximation	6
A. Hubbard-Stratonovich transformation	6
B. Mean-field Majorana single-particle Hamiltonian	7
C. Integrating out the Majorana fields	8
D. Mean-field gap equations	9
E. Approximate mean-field gap equations	10
F. Hessian at the saddle points	11
G. Interpretation	12
IV. Beyond mean-field theory: Dimensional crossover from a random phase approximation	13
V. Two-dimensional Majorana fermions, one-dimensional solitons	16
VI. A single two-leg ladder	18
A. Microscopic lattice model and its continuum limit	18
B. Abelian bosonization	20
C. Majorana representation	21
VII. Coupled two-leg ladders	22
A. Microscopic lattice model and its continuum limit	22
B. Majorana representation	24
C. Abelian bosonization	26
D. Spontaneous symmetry breaking	28
E. Competing instabilities	29

VIII. Summary	30
Acknowledgments	30
References	30

I. INTRODUCTION AND RESULTS

A. Motivation

Most of the observed low-temperature phases in condensed matter physics are characterized by spontaneous symmetry breaking (SSB) through the onset of a local order parameter acquiring a non-vanishing expectation value. Antiferromagnetism is the paradigmatic example of SSB with the staggered magnetization as the local order parameter. On the other hand, it has been found that such states as exist in the fractional quantum Hall effect (FQHE) possess a hidden (topological) order not associated with any local order parameter. This type of order may exist only if the bulk is incompressible, in which case it reveals itself in several ways. In particular, a sufficient condition for the topological order is the existence of robust gapless boundary excitations. If the system is situated on a manifold without boundaries, the ground state is degenerate and the degeneracy depends on the genus of the manifold. These characteristics of topological order were formulated by Wen in Ref. 1, but the notion has been later refined by relating it to the presence of long-range quantum entanglement in Refs. 2–4. The other feature in $(2+1)$ -dimensional spacetime is the presence of gapped point-like excitations obeying braiding statistics that is neither fermionic nor bosonic. This sharpening of what constitutes the essence of topological order in $(2+1)$ -dimensional spacetime has opened the possibility of its classification.^{5,6} However, these discussions of topological order have been conducted with little reference to microscopic models. There are very few of

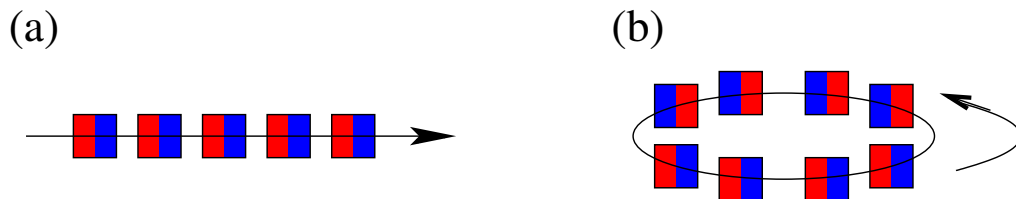


FIG. 1. (Color online) (a) Alignment of blocks along an open line. Each block represents a non-chiral conformal field theory in $(1+1)$ -dimensional spacetime. One half of the gapless modes are left movers, the other half are right movers. This partition into movers with opposite chirality is represented by the coloring blue and red, respectively. (b) Alignment of blocks along a circle.

them which can be treated by controlled approximations; most notably the quantum dimer model on the triangular lattice⁷ and the Kitaev model on the honeycomb lattice⁸. The latter is a model of interacting quantum spins, whose excitations are Majorana fermions. Their propagation is facilitated by the presence of the so-called visons which in this model are immobile \mathbb{Z}_2 gauge field fluxes.

One way to construct microscopic models with topological order is to use the so-called wire construction. The idea, following Kane and his collaborators,^{9–12} is to couple elementary building blocks that realize a conformal field theory (CFT) in $(1+1)$ -dimensional spacetime [by construction this building block cannot be gapped into a phase supporting topological order in $(1+1)$ -dimensional spacetime] so as to realize an incompressible phase of matter in $(d+1)$ -dimensional spacetime that supports topological order. Although, the diagnostic for topological order is a degeneracy of the ground-state manifold that depends on the genus of compactified space, it is more convenient to use a stronger (a sufficient but not necessary) condition for topological order, namely, the existence of protected gapless boundary states that are localized on the $(d-1)$ -dimensional boundaries of $d > 1$ -dimensional space. It is then suggested to weakly couple these building blocks so as to gap the bulk while leaving the boundaries gapless. A generic coupling between these building blocks will not do that, for such a coupling can yield three possible outcomes. First, the resulting phase of matter in $(d+1)$ -dimensional spacetime may be gapless and ordered. This is what happens when antiferromagnetic spin-1/2 chains are coupled so as to realize an antiferromagnetic square lattice.^{13–15} Second, the resulting phase of matter in $(d+1)$ -dimensional spacetime may be gapful, but without topological order. This is what happens when antiferromagnetic spin-1/2 chains are weakly coupled pairwise so as to realize a stacking of two-leg ladders which, in turn, are even more weakly coupled pairwise.¹⁶ We are interested in the third outcome, namely, when the resulting phase of matter in $(d+1)$ -dimensional spacetime is incompressible and supports topological order. Which outcome is realized is determined by the choice of the couplings between the building blocks, that is by the energetics.

In this paper we will be dealing with a model in two-dimensional space. In this case, a sufficient but not neces-

sary condition for topological order is that in the infrared limit (i) the first and last building blocks acquire a nonvanishing yet reduced central charge when their direct coupling is forbidden by locality (open boundary conditions along the stacking direction), whereas (ii) the ground state is fully gapped when their direct coupling is compatible with locality (closed boundary conditions along the stacking direction). This situation is pictured in Fig. 1. Each block represents some given non-chiral CFT in $(1+1)$ -dimensional spacetime. The stacking direction of the blocks is oriented by the arrow. The coloring red and blue represents the left- and right-movers from the CFT, respectively. It is possible to gap out a pair of movers of opposite chirality belonging to two consecutive blocks by coupling in a local way the right movers from a block to the left movers of the nearest-neighbor block along the stacking direction. This leaves the left movers from the first block and the right movers from the last block gapless in panel (a) from Fig. 1, whereas all states are gapped when periodic boundary conditions are imposed as in panel (b) from Fig. 1. The challenge is to realize Fig. 1 by appealing only to local couplings between the microscopic degrees of freedom such as lattice electrons or magnetic moments. This challenge was met for all symmetry classes from the ten-fold way in Ref. 17, where it was shown that five of them can support Abelian topological order (ATO) upon choosing local (electronic) interactions between consecutive blocks.

A proposal to realize a spin liquid supporting chiral edge states with non-integer valued central charges was given in Refs. 18 and 19. It is the fractional part to the chiral central charge of the edge states that signals the non-Abelian topological order (NATO). This proposal relies on local interactions within and between consecutive blocks from Fig. 1 that are both marginally relevant and compete with each other. Consequently, it could not be proven that all states are gapped when periodic boundary conditions are imposed as in panel (b) from Fig. 1. The purpose of this paper is to modify the field theory studied in Ref. 19 to rule out the possibility that the flow to strong coupling in Ref. 19, when periodic boundary conditions are imposed as in panel (b) from Fig. 1, delivers a gapless phase of matter. This modification makes the theory amenable to a mean-field approximation that predicts two gapped phases separated by a gap-closing tran-

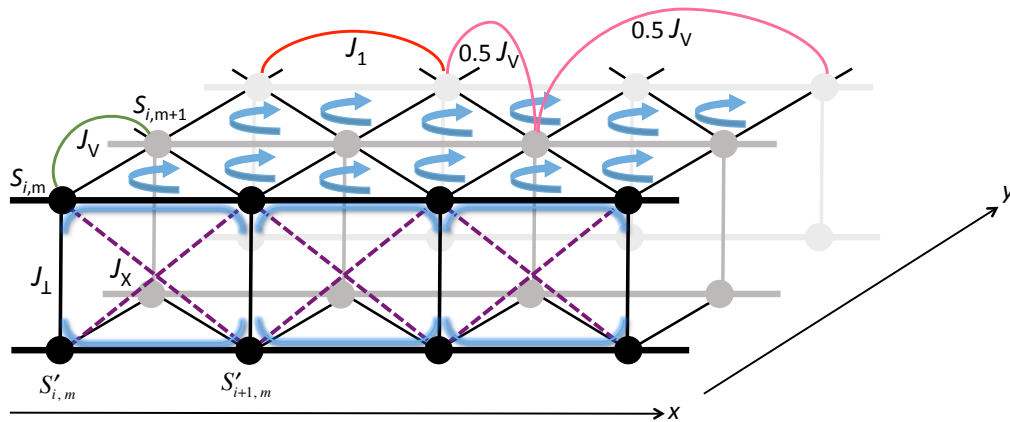


FIG. 2. (Color online) Coupled quantum spin-1/2 two-leg ladders that realize the Ising topological order in two-dimensional space. The intra-ladder couplings J_1 , J_\perp , $J_x = -J_\perp/2$, and J_U (represented by the blue curly bracket) are defined in Eq. (6.1). The inter-ladder couplings J_V (represented by the green bond), $J_V/2$ (represented by the magenta bond), and J_x (represented by the blue arrows) are defined in Eq. (7.1). The lattice geometry can also be thought of as that of a bilayer of two square lattices.

sition when the couplings between consecutive blocks are chosen to be marginally relevant. One gapped phase supports ATO. The other gapped phase supports NATO. We also find a third gapless phase, a two-dimensional sliding Luttinger phase when the couplings between consecutive blocks are chosen to be marginally irrelevant.

B. Results and outline

As was the case with Ref. 19, we shall take the blocks from Fig. 1 to realize an Ising CFT on the boundary, i.e., a CFT with central charge $c = 1/2$. However, unlike in Ref. 19 where this Ising CFT was driven by marginal perturbations to a CFT with central charge $c = 2$, in this paper the Ising CFT is driven by a strongly relevant perturbation. This distinction gives a much better control on the strong coupling fixed point that realizes the Ising NATO when two consecutive blocks are coupled through interactions.

Throughout this paper, we are mostly preoccupied with the analysis of the field theory corresponding to Fig. 1. The choice of a microscopic theory delivering the Ising criticality is dictated by simplicity at the level of CFT rather than by simplicity on the microscopic level. This microscopic theory is a quantum spin-1/2 ladder, whose low-energy effective field theory is depicted by any one of the single square box colored in red and blue in Fig. 1. This was also the case in Ref. 19. However, instead of relying on two-body spin-1/2 interactions which are reduced to marginal current-current interactions at low energies, as was the case in Ref. 19, we shall rely in this paper on four-body spin-1/2 interactions which are reduced to a mass term for three out of the four gapless Majorana fields that encode the critical theory of two decoupled antiferromagnetic quantum spin-1/2 chains. Once a single

spin-1/2 ladder is tuned to the Ising critical point, we couple the ladders as was done in Ref. 19. The resulting lattice model is depicted in Fig. 2. Each ladder viewed from the side in Fig. 2 is represented by a square box colored in red and blue in Fig. 1 at low energies.

The lattice model for a single spin-1/2 ladder is defined in Sec. VI. The lattice model for a one-dimensional array of coupled spin-1/2 ladders is defined in Sec. VII. Its continuum limit is derived and shown to agree with the Majorana Hamiltonian (2.1).

The continuum limit is derived under the assumption that one can eliminate couplings between the most relevant fields on consecutive ladders and neglect those between more distant ladders. Then, at low energies, the coupled quantum spin-1/2 ladders in Fig. 2 admit an effective description in terms of an interacting quantum field-theory with four Majorana fields per ladder. Dealing with the fermionic field theory, one has to remember that its Hilbert space is greater than the one of the original spin model. In particular, it allows states created by odd numbers of Majorana fermions per ladder. There are no such states in the spin model. This fermionic field theory is the starting point captured by Eq. (2.1) from Sec. II. In this mapping the Majorana fields carry a flavor index $m = 1, \dots, n$ that labels the quantum spin-1/2 ladders. The kinetic energy of the Majorana fields is encoded by a Wess-Zumino-Novikov-Witten (WZNW) action $\hat{\mathcal{H}}_{\text{WZNW}}$. This kinetic energy ignores all inter-ladder interactions and treats any one of the ladders as two decoupled antiferromagnetic quantum spin-1/2 chains, each of which is at an $SU(2)_1$ quantum critical point. The intra-ladder interactions between the quantum spin-1/2 turn at low energies into bare masses $m_\mu \in \mathbb{R}$ ($\mu = 0, 1, 2, 3$) for each Majorana field. The inter-ladder interactions between the quantum spin-1/2 turn at low energies into an $O(4)$ -symmetric interaction

that couples Majorana fields belonging to two consecutive ladders. This interaction resembles the Gross-Neveu interaction, and we shall call it a Gross-Neveu-like interaction.

We treat the $O(4)$ -symmetric Gross-Neveu-like interaction by two alternative methods. In Sec. III A, we use the mean field procedure based on decoupling of the four-fermion interaction by means of the Hubbard-Stratonovich transformation. In Secs. IV and V, we use the approach which is based on combination of non-perturbative results extracted from the exact solution of the $O(4)$ -symmetric Gross-Neveu model and Random Phase approximation. The phase diagram from Fig. 3 is conjectured from a mean-field approximation that we derive in the remainder of Sec. III. In Fig. 3, λ denotes the coupling of the non-Abelian current-current interactions between consecutive blocks. This interaction is either marginally irrelevant for negative λ or marginally relevant for positive λ . The mean-field phase diagram in Fig. 5 is parametrized by m_t and the mean-field value of the spectral gap $|\phi(\lambda)|/2$ under the assumption that the so-called singlet Majorana is gapless, $m_0 \equiv m_s = 0$, while a triplet of Majoranas have the isotropic mass $m_a \equiv m_t$ for $a = 1, 2, 3$. There exist mean-field critical lines that correspond to the condition $|\phi(\lambda)|/2 = |m_t|$ along which the mean-field Majorana gap vanishes. The regions $|\phi(\lambda)|/2 > |m_t|$ and $|\phi(\lambda)|/2 < |m_t|$ correspond to phases of matter supporting NATO and ATO, respectively.

From the mean-field phase diagram in Fig. 5, we conjecture the phase diagram in Fig. 3 that is parametrized by the inter-ladder interaction with the uniform coupling λ and by the triplet mass m_t . The bare value of the triplet mass is a function of the microscopic magnetic couplings of any one of the ladders. For $\lambda > 0$, the $O(4)$ -symmetric Gross-Neveu-like interaction guarantees a non-vanishing value for the mean-field $\phi(\lambda)$. On the other hand, for $\lambda < 0$, the $O(4)$ Gross-Neveu-like interaction also guarantees that the mean-field $\phi(\lambda)$ vanishes. The line $m_t = 0$ is exactly solvable and we use this solution in IV. The dashed green line in Fig. 3 corresponds to the mean-field transition line. The phases NATO and ATO in Fig. 3 correspond to the mean-field regions $|\phi(\lambda)|/2 > |m_t|$ and $|\phi(\lambda)|/2 < |m_t|$, respectively.

The nonvanishing mean-field values for $\phi(\lambda)$ follow from integrating over the Majorana fields in Sec. III C and deriving a mean field equation obeyed by $\phi(\lambda)$ in Sec. III D.

In Secs. IV and V, we establish the form of the bulk excitation spectrum. It consists of Majorana fermions propagating in two spatial dimensions and visons excitations which can propagate only along chains. As far as we are aware this is the only microscopic model (besides the Kitaev one) where such particles have been rigorously obtained.

As we have mentioned above, the lattice model for a single spin-1/2 ladder is defined in Sec. VI, where we also derive its continuum limit. The lattice model for a one-

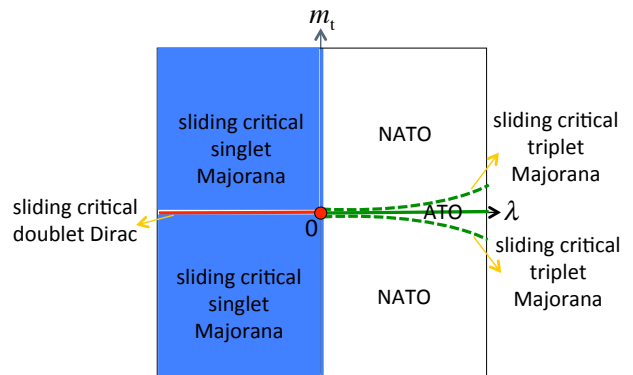


FIG. 3. (Color online) Conjectured phase diagram of the theory (2.1) with $m_0 = 0$ and $m_a = m_t$ for $a = 1, 2, 3$.

dimensional array of coupled spin-1/2 ladders is defined in Sec. VII. We then discuss its continuum limit, which is the Majorana Hamiltonian (2.1). We conclude with a summary in Sec. VIII.

II. MAJORANA FIELD THEORY

A. Definition

We begin with

$$\hat{\mathcal{H}} := \hat{\mathcal{H}}_0 + \hat{\mathcal{H}}_{\text{intra-ladder}} + \hat{\mathcal{H}}_{\text{inter-ladder}}, \quad (2.1a)$$

$$\hat{\mathcal{H}}_0 = \sum_{m=1}^n \sum_{\mu=0}^3 \frac{i}{2} v_{\mu} \left(\hat{\chi}_{L,m}^{\mu} \partial_x \hat{\chi}_{L,m}^{\mu} - \hat{\chi}_{R,m}^{\mu} \partial_x \hat{\chi}_{R,m}^{\mu} \right), \quad (2.1b)$$

$$\hat{\mathcal{H}}_{\text{intra-ladder}} = \sum_{m=1}^n \sum_{\mu=0}^3 i m_{\mu} \hat{\chi}_{L,m}^{\mu} \hat{\chi}_{R,m}^{\mu}, \quad (2.1c)$$

$$\hat{\mathcal{H}}_{\text{inter-ladder}} = \sum_{m=1}^{n-1} \frac{\lambda}{4} \left(\sum_{\mu=0}^3 \hat{\chi}_{L,m}^{\mu} \hat{\chi}_{R,m+1}^{\mu} \right)^2, \quad (2.1d)$$

where the velocities v_{μ} , the masses m_{μ} , and the coupling λ are all real valued. The quantum fields obey the Majorana equal-time anti-commutators

$$\left\{ \hat{\chi}_{M,m}^{\mu}(x), \hat{\chi}_{M',m'}^{\mu'}(x') \right\} = \delta_{MM'} \delta_{mm'} \delta_{\mu\mu'} \delta(x - x'), \quad (2.1e)$$

where $\mu = 0, 1, 2, 3$ labels a quartet of Majorana fields, $M = L, R$ denotes the left- and right-movers, and $m, m' = 1, \dots, n$ is the ladder index. Hamiltonian (2.1) has the following symmetries.

First, the μ -resolved fermion parity is conserved owing to the symmetry of Hamiltonian (2.1) under the Ising-like transformation

$$\hat{\chi}_{M,m}^{\mu}(x) \mapsto \sigma^{\mu} \hat{\chi}_{M,m}^{\mu}(x), \quad \sigma^{\mu} = \pm 1, \quad (2.2)$$

for any $\mu = 0, \dots, 3$, $M = L, R$, $m = 1, \dots, n$, and $0 \leq x \leq L_x$.

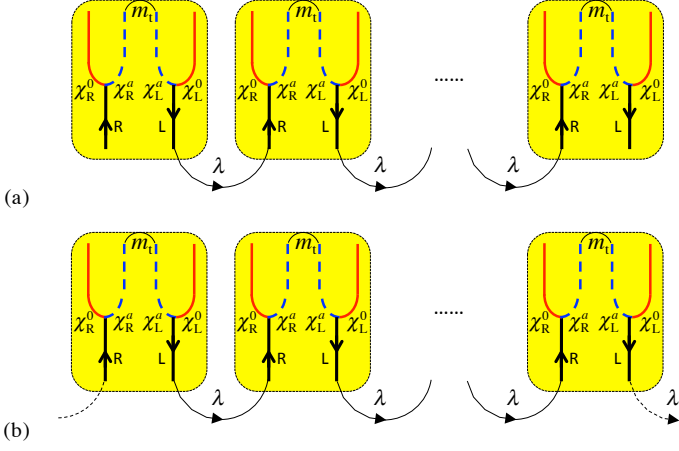


FIG. 4. (Color online) (a) A pictorial representation of the theory (2.1) with $m_0 = 0$ and $m_a = m_t$ for $a = 1, 2, 3$ when open boundary conditions (OBC) are imposed along the y direction. (b) A pictorial representation of the theory (2.1) with $m_0 = 0$ and $m_a = m_t$ for $a = 1, 2, 3$ when periodic boundary conditions (PBC) are imposed along the y direction.

Second, Hamiltonian (2.1) is invariant under the m -resolved \mathbb{Z}_2 transformation by which

$$\widehat{\chi}_{M,m}^\mu(x) \mapsto \sigma_m \widehat{\chi}_{M,m}^\mu(x), \quad \sigma_m = \pm 1, \quad (2.3)$$

for any $\mu = 0, \dots, 3$, $M = L, R$, $m = 1, \dots, n$, and $0 \leq x \leq L_x$.

We observe that $\widehat{\mathcal{H}}_0$ defined by Eq. (2.1b) is $O(4)$ symmetric if $v_\mu \equiv v$ is independent of μ , $\widehat{\mathcal{H}}_{\text{intra-ladder}}$ defined by Eq. (2.1c) is $O(4)$ symmetric if $m_\mu \equiv m$ is independent of μ , and $\widehat{\mathcal{H}}_{\text{inter-ladder}}$ defined by Eq. (2.1d) is $O(4)$ symmetric. This global $O(4) = \mathbb{Z}_2 \times SO(4)$ symmetry encodes the global $\mathbb{Z}_2 \times SU(2) \times SU(2)$ symmetry of the microscopic inter-ladder interactions depicted in Fig. 2, as will be explained in more details in Secs. VI and VII.

B. Limiting cases

In this subsection, we consider the following limiting cases for the theory defined by Eq. (2.1) under the assumptions that

$$\begin{aligned} v_0 &\equiv v_s, & m_0 &\equiv m_s = 0, \\ v_a &\equiv v_t, & m_a &\equiv m_t, \quad a = 1, 2, 3. \end{aligned} \quad (2.4)$$

A cartoon picture of the theory (2.1) with these assumptions is depicted in Fig. 4(a).

Case $\lambda = 0$ and $m_t \neq 0$. There are n gapless helical Majorana fields $\widehat{\chi}_{L,m}^0$ and $\widehat{\chi}_{R,m}^0$ for $m = 1, \dots, n$ that propagate in opposite directions in each bundle m . The two-dimensional system is critical in the singlet Majorana sector where it realizes a sliding Luttinger phase. This

case corresponds to the vertical axis of the conjectured phase diagram in Fig. 3.

Case $\lambda \neq 0$ and $m_t = 0$. The Hamiltonian (2.1) simplifies to

$$\widehat{\mathcal{H}} := \widehat{\mathcal{H}}_{\text{edge-states}, m=1} + \widehat{\mathcal{H}}_{\text{edge-states}, m=n} + \sum_{m=1}^{n-1} \widehat{\mathcal{H}}_{\text{GN}, m}, \quad (2.5a)$$

$$\widehat{\mathcal{H}}_{\text{edge-states}, m=1} := \sum_{\mu=0}^3 \frac{i}{2} v_\mu \left(-\widehat{\chi}_{R, m=1}^\mu \partial_x \widehat{\chi}_{R, m=1}^\mu \right), \quad (2.5b)$$

$$\widehat{\mathcal{H}}_{\text{edge-states}, m=n} := \sum_{\mu=0}^3 \frac{i}{2} v_\mu \left(+\widehat{\chi}_{L, m=n}^\mu \partial_x \widehat{\chi}_{L, m=n}^\mu \right), \quad (2.5c)$$

$$\begin{aligned} \widehat{\mathcal{H}}_{\text{GN}, m} &:= \sum_{\mu=0}^3 \frac{i}{2} v_\mu \left(\widehat{\chi}_{L, m}^\mu \partial_x \widehat{\chi}_{L, m}^\mu - \widehat{\chi}_{R, m+1}^\mu \partial_x \widehat{\chi}_{R, m+1}^\mu \right) \\ &+ \frac{\lambda}{4} \left(\sum_{\mu=0}^3 \widehat{\chi}_{L, m}^\mu \widehat{\chi}_{R, m+1}^\mu \right)^2. \end{aligned} \quad (2.5d)$$

Here, the four-Majorana interaction in Eq. (2.5d) is an $O(4)$ -symmetric interaction of the Gross-Neveu type.

The m -resolved symmetry (2.3) of Hamiltonian (2.5) is enhanced to the invariance under the M - and m -resolved \mathbb{Z}_2 transformation

$$\widehat{\chi}_{M,m}^\mu(x) \mapsto \sigma_{M,m} \widehat{\chi}_{M,m}^\mu(x), \quad \sigma_{M,m} = \pm 1, \quad (2.6)$$

for any $\mu = 0, \dots, 3$, $M = L, R$, $m = 1, \dots, n$, and $0 \leq x \leq L_x$. Indeed, whereas any transformation (2.6) changes

$$\widehat{\phi}_{m, m+1} := \lambda \sum_{\mu=0}^3 i \widehat{\chi}_{L, m}^\mu \widehat{\chi}_{R, m+1}^\mu \quad (2.7)$$

according to the rule

$$\widehat{\phi}_{m, m+1} \mapsto \sigma_{L, m} \sigma_{R, m+1} \widehat{\phi}_{m, m+1}, \quad (2.8)$$

it leaves $\widehat{\phi}_{m, m+1}^2$ unchanged. Any one of these M - and m -resolved symmetries obeying the conditions $\sigma_{L, m} \sigma_{R, m+1} = -1$ and either $\sigma_{L, m} = -\sigma_{R, m}$ or $\sigma_{L, m+1} = -\sigma_{R, m+1}$ for some m is broken if any one of the masses m_μ is non-vanishing. This enhanced symmetry relative to the symmetry (2.3) reflects the fact that the limit with all masses m_μ vanishing is nothing but n decoupled Hamiltonians, each of which represents a pair of interacting non-chiral Majorana fields evolving in $(1+1)$ -dimensional spacetime.

In this limit, Hamiltonian (2.5) is known²⁰ to be integrable and gapped (gapless) when $v_\mu = v$ with $\mu = 0, 1, 2, 3$ and $\lambda > 0$ ($\lambda < 0$). Thus, we should further distinguish between the following two cases.

Case $\lambda > 0$. The bulk is gapped with the four gapless chiral Majorana edge modes $\widehat{\chi}_{R, m=1}^\mu$ and $\widehat{\chi}_{L, m=n}^\mu$. Since

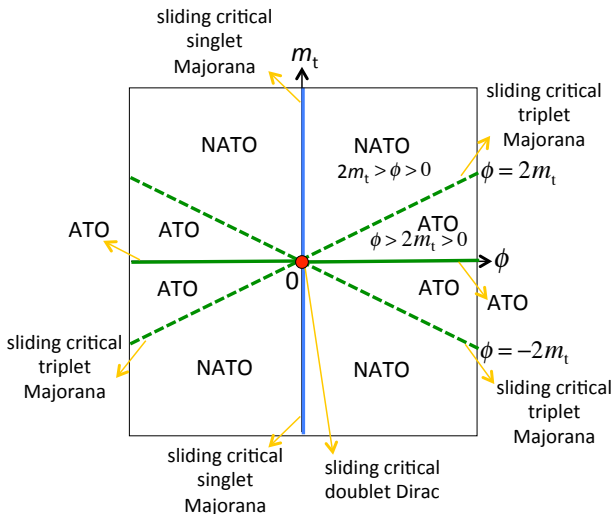


FIG. 5. (Color online) The mean-field phase diagram presented in terms of m_t and the mean-field value ϕ under the condition of $m_0 = 0$ and $m_a = m_t$ for $a = 1, 2, 3$.

the chiral central charge of each edge is two, the corresponding bulk hosts an ATO. This case corresponds to the positive horizontal-axis (represented by the solid green line) of the conjectured phase diagram in Fig. 3.

Case $\lambda < 0$. The four pairs of gapless helical Majorana fields $\hat{\chi}_{L,m}^\mu$ and $\hat{\chi}_{R,m}^\mu$ with $\mu = 0, 1, 2, 3$ are freely propagating in each ladder $m = 1, \dots, n$. The two-dimensional bulk is critical and shares the same universality class as a sliding Luttinger phase. This case corresponds to the negative horizontal-axis (represented by the solid red line) of the conjectured phase diagram in Fig. 3.

Case $\lambda < 0$ and $m_t \neq 0$. We conjecture that, since the Gross-Neveu interaction with $\lambda < 0$ is marginally irrelevant, the resulting theory is the same as the case of $\lambda = 0$ and $m_t \neq 0$. This case corresponds to the blue colored region of the conjectured phase diagram in Fig. 3.

Case $\lambda > 0$ and $m_t \neq 0$. We conjecture the competition between two phases, an ATO phase and a NATO phase separated by a bulk gap closing transition (represented by the dashed green lines in Fig. 3). This conjecture will be verified within a mean-field approximation.

III. MEAN-FIELD APPROXIMATION

We are going to carry out a mean-field calculation from which we deduce the mean-field phase diagram in Fig. 5. Afterwards, we establish the conjectured phase diagram in Fig. 3.

Our strategy does not rely on the $O(4)$ symmetry of the Gross-Neveu-like interaction, it can generically be broken by anisotropic singlet (v_s) and triplet (v_t) velocities, i.e.,

$$v_s \neq v_t. \quad (3.1)$$

If we decouple the Gross-Neveu-like interaction in an $O(4)$ -symmetric way through a scalar field ϕ , then a uniform and non-vanishing expectation value for ϕ provides the singlet and triplet Majoranas with an $O(4)$ -symmetric mean-field mass.

In the process of solving the mean-field gap equation (3.32a), we shall be primarily interested with the case $m_s = 0$ for which the decoupled ladders are fine-tuned to an Ising critical point. In Fig. 3, we identify the regions from the $\lambda - m_t$ plane for which the mean-field single-particle singlet gap is non-vanishing when periodic boundary conditions (PBC) are imposed.

A. Hubbard-Stratonovich transformation

We proceed with some manipulations on the partition function

$$Z := \text{Tr} \exp \left(-\beta \int_0^{L_x} dx \hat{\mathcal{H}} \right), \quad (3.2)$$

where β is the inverse temperature, the trace is over the Fock space spanned by the Majorana fields, and $\hat{\mathcal{H}}$ was defined in Eq. (2.1). We can manipulate the inter-ladder current-current interaction (2.1d) by introducing an auxiliary scalar field. This we do using the path-integral representation of the partition function.

We work in two-dimensional Euclidean spacetime and use the path-integral representation of our model. Periodic boundary conditions are imposed in space across the rectangle of area $L_x \times L_y$. We shall denote by $\alpha_y \equiv 1/\Lambda_y$ the separation between two consecutive ladders. We shall denote by $\alpha_x \equiv 1/\Lambda_x$ the ultraviolet cutoff along the ladders. The boundary conditions along the imaginary-time segment $[0, \beta[$ are periodic for bosonic fields and antiperiodic for Grassmann-valued fields. The model is defined by

$$Z := \int \mathcal{D}[\phi] \int \mathcal{D}[\chi^0, \chi^1, \chi^2, \chi^3] e^{-S}, \quad (3.3a)$$

$$S := \int_0^\beta d\tau \int_0^{L_x} dx \sum_{m=1}^{L_y/\alpha_y} (\mathcal{L}_{\chi,m} + \mathcal{L}_{\phi,m} + \mathcal{L}_{\chi,\phi,m}), \quad (3.3b)$$

$$\begin{aligned} \mathcal{L}_{\chi,m} := & \frac{1}{2} \sum_{\mu=0}^3 \left[\chi_{L,m}^\mu (\partial_\tau + iv_\mu \partial_x) \chi_{L,m}^\mu \right. \\ & \left. + \chi_{R,m}^\mu (\partial_\tau - iv_\mu \partial_x) \chi_{R,m}^\mu \right], \end{aligned} \quad (3.3c)$$

$$\mathcal{L}_{\phi,m} := \frac{1}{4\lambda} (\phi_{m,m+1})^2, \quad (3.3d)$$

$$\begin{aligned} \mathcal{L}_{\chi,\phi,m} := & \sum_{\mu=0}^3 i m_\mu \chi_{L,m}^\mu \chi_{R,m}^\mu \\ & + \sum_{\mu=0}^3 \frac{1}{2} \left(-i \chi_{L,m}^\mu \chi_{R,m+1}^\mu \right) \phi_{m,m+1}. \end{aligned} \quad (3.3e)$$

Here, the engineering dimensions of the Majoranas are length^{-1/2}, the engineering dimensions of the auxiliary bosonic fields are length⁻¹, and the engineering dimensions of the couplings λ are length⁰. The action (3.3b) has the following symmetries.

First, the μ -resolved Majorana parity is conserved owing to the symmetry of S defined in Eq. (3.3b) under the Ising-like transformation

$$\chi_{M,m}^\mu(\tau, x) \mapsto \sigma^\mu \chi_{M,m}^\mu(\tau, x), \quad \sigma^\mu = \pm 1, \quad (3.4)$$

for any $\mu = 0, \dots, 3$, $M = L, R$, $m = 1, \dots, n$, $0 \leq \tau \leq \beta$, and $0 \leq x \leq L_x$.

Second, action (3.3b) is invariant under the m -resolved Ising-like transformation

$$\begin{aligned} \chi_{M,m}^\mu(\tau, x) &\mapsto \sigma_m \chi_{M,m}^\mu(\tau, x), & \sigma_m &= \pm 1, \\ \phi_{m,m+1}(\tau, x) &\mapsto \sigma_m \sigma_{m+1} \phi_{m,m+1}(\tau, x), \end{aligned} \quad (3.5)$$

for any $\mu = 0, \dots, 3$, $M = L, R$, $m = 1, \dots, n$, $0 \leq \tau \leq \beta$, and $0 \leq x \leq L_x$.

The m -resolved symmetry (3.5) of the action (3.3b) is enhanced in the massless limit $m_\mu = 0$ for $\mu = 0, 1, 2, 3$ to the M - and m -resolved symmetry under the transformation

$$\begin{aligned} \chi_{M,m}^\mu(\tau, x) &\mapsto \sigma_{M,m} \chi_{M,m}^\mu(\tau, x), & \sigma_{M,m} &= \pm 1, \\ \phi_{m,m+1}(\tau, x) &\mapsto \sigma_{L,m} \sigma_{R,m+1} \phi_{m,m+1}(\tau, x), \end{aligned} \quad (3.6)$$

for any $\mu = 0, \dots, 3$, $M = L, R$, $m = 1, \dots, n$, $0 \leq \tau \leq \beta$, and $0 \leq x \leq L_x$. Any non-vanishing mass m_μ reduces the M - and m -resolved symmetry of the action (3.3b) to the m -resolved symmetry (3.5).

B. Mean-field Majorana single-particle Hamiltonian

To proceed, we assume that the scalar fields are independent of spacetime and of the index m , i.e.,

$$\phi_{m,m+1}(\tau, x) \equiv \phi, \quad S_\phi = \beta L_x \frac{L_y}{a_y} \frac{1}{4\lambda} \phi^2. \quad (3.7)$$

This assumption implies translation symmetry in spacetime. Hence, we introduce the Fourier transformations

$$\chi_{M,m}^\mu(\tau, x) = \sqrt{\frac{a_y}{\beta L_x L_y \omega_{\omega, k_x, k_y}}} \sum e^{-i(k_x x + k_y m a_y - \omega \tau)} \chi_{M,\omega, \mathbf{k}}^\mu \quad (3.8a)$$

with the reality condition

$$\chi_{M,\omega, \mathbf{k}}^{\mu*} = \chi_{M,-\omega, -\mathbf{k}}^\mu \quad (3.8b)$$

for $\mu = 0, 1, 2, 3$, $M = L, R$, and $m = 1, \dots, L_y/a_y$. We shall make use of the identity

$$\begin{aligned} \int_0^\beta d\tau \int_0^{L_x} dx \sum_{m=1}^{L_y/a_y} \chi_{L,m}^\mu \chi_{R,m+1}^\mu = \\ \sum_{\omega, \mathbf{k}} e^{-i k_y a_y} \chi_{L,-\omega, -\mathbf{k}}^\mu \chi_{R,\omega, \mathbf{k}}^\mu \end{aligned} \quad (3.9)$$

for any $\mu = 0, 1, 2, 3$. We should emphasize that we have imposed periodic boundary condition along the y -direction

$$\chi_{M,n+1}^\mu \equiv \chi_{M,1}^\mu, \quad M = L, R, \quad (3.10)$$

when we perform the Fourier transformation. This amounts to extending the upper limit for the summation from $n-1$ to n in the original inter-ladder Hamiltonian (2.1d). This choice of boundary conditions is depicted in Fig. 4(b). If so,

$$\begin{aligned} S_\chi + S_{\chi, \phi} &\equiv \int_0^\beta d\tau \int_0^{L_x} dx \sum_{m=1}^{L_y/a_y} (\mathcal{L}_{\chi, m} + \mathcal{L}_{\chi, \phi, m}) \\ &= \sum_{\omega, \mathbf{k}} \sum_{\mu=0}^3 \frac{1}{2} (\chi_{R,-\omega, -\mathbf{k}}^\mu \chi_{L,-\omega, -\mathbf{k}}^\mu) \begin{pmatrix} i\omega - v_\mu k_x & -i(m_\mu - e^{+i k_y a_y} \frac{1}{2} \phi) \\ i(m_\mu - e^{-i k_y a_y} \frac{1}{2} \phi) & i\omega + v_\mu k_x \end{pmatrix} \begin{pmatrix} \chi_{R,\omega, \mathbf{k}}^\mu \\ \chi_{L,\omega, \mathbf{k}}^\mu \end{pmatrix}. \end{aligned} \quad (3.11a)$$

The mean-field Majorana single-particle Hamiltonian is defined by

$$\widehat{H}_{\mathbf{k}}^{\text{MF}} := \sum_{\mu=0}^3 \widehat{H}_{\mu, \mathbf{k}}^{\text{MF}}, \quad (3.11b)$$

where

$$\widehat{H}_{\mu, \mathbf{k}}^{\text{MF}} := \frac{1}{2} \begin{pmatrix} -v_\mu k_x & -i(m_\mu - e^{+i k_y a_y} \frac{\phi}{2}) \\ i(m_\mu - e^{-i k_y a_y} \frac{\phi}{2}) & v_\mu k_x \end{pmatrix}. \quad (3.11c)$$

Thus, there are eight branches of mean-field excitations with the dispersions (under the assumption that ϕ is real valued)

$$\varepsilon_{\mu,\pm}(k_x, k_y) = \pm \frac{1}{2} \sqrt{v_\mu^2 k_x^2 + m_\mu^2 + \frac{\phi^2}{4} - m_\mu \phi \cos(k_y \mathbf{a}_y)}, \quad (3.12)$$

for $\mu = 0, \dots, 3$. The mean-field gaps are non-vanishing if and only if

$$m_\mu - e^{\pm i k_y \mathbf{a}_y} \frac{\phi}{2} \neq 0. \quad (3.13)$$

More specifically, the mean-field Majorana gap around $(k_x = 0, k_y = 0)$ and $(k_x = 0, k_y = \pi)$ are, for $\mu = 0, \dots, 3$,

$$\varepsilon_{\mu,+}(0, 0) - \varepsilon_{\mu,-}(0, 0) = \left| m_\mu - \frac{\phi}{2} \right|, \quad (3.14a)$$

and

$$\varepsilon_{\mu,+}(0, \pi) - \varepsilon_{\mu,-}(0, \pi) = \left| m_\mu + \frac{\phi}{2} \right|, \quad (3.14b)$$

respectively. The mean-field gap (3.14a) and (3.14b) is the smallest gap when $\text{sgn}(m_\mu \phi) = +$ and $\text{sgn}(m_\mu \phi) = -$, respectively.

For any non-vanishing mean-field Majorana gap Δ_μ

$$\Delta_\mu := \left| m_\mu - \frac{|\phi|}{2} \right|, \quad (3.15)$$

the flavor μ realizes an insulating phase. Whether this insulating phase is trivial (no protected edge state when OBC are imposed along the y -direction) or non-trivial (existence of protected edge states when OBC are imposed along the y -direction) depends on the relative magnitude of $|m_\mu|$ with respect to the mean-field value $|\phi|/2$. The flavor μ realizes a topologically trivial insulating phase if

$$|m_\mu| > \frac{|\phi|}{2}, \quad (3.16a)$$

while it realizes a topologically non-trivial insulating phase if

$$|m_\mu| < \frac{|\phi|}{2}. \quad (3.16b)$$

The criteria (3.16) for the topological non-trivial and trivial phases can be understood as follows. In the limit $|m_\mu|/|\phi| = \infty$, the single-particle mean-field Hamiltonian is gapped by pairing left- and right-moving Majorana modes in one ladder at a time. By construction there is no edge state. This is the topologically trivial insulator. In the opposite limit of $|m_\mu|/|\phi| = 0$, not all Majorana modes are paired. A pair of Majorana modes with opposite chiralities remains free to propagate in the first and last ladder. A phase transition should occur

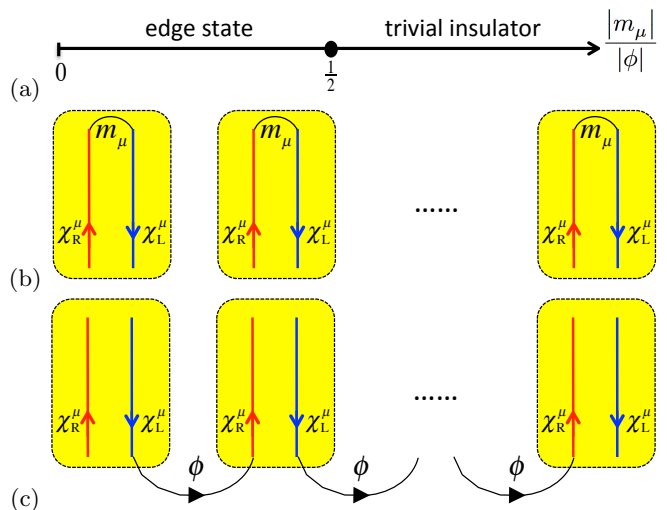


FIG. 6. (Color online) (a) Flavor(μ)-resolved phase diagram for the single-particle mean-field Hamiltonian as a function of $|m_\mu|/|\phi|$. The topologically trivial insulating phase in the limit $|m_\mu|/|\phi| = \infty$ is depicted in panel (b). The topologically non-trivial insulating phase in the limit $|m_\mu|/|\phi| = 0$ is depicted in panel (c). A phase transition should occur when $|m_\mu|/|\phi|$ is of order 1/2. (b) When $\phi = 0$ and $m_\mu \neq 0$, the single-particle mean-field Hamiltonian is gapped by pairing left- and right-moving Majorana modes in one ladder at a time. By construction there is no edge state. This is the topologically trivial insulator. (c) When $m_\mu = 0$ and $\phi \neq 0$, not all Majorana modes are paired. A pair of Majorana modes with opposite chiralities remains free to propagate in the first and last ladder. This is the topologically non-trivial insulator.

when $|m_\mu|/|\phi|$ is of order 1/2. Figure 6 captures the essence of this criterion.

Once it is established that ϕ is non-vanishing, the resulting central charge of the edge states depends on how many m_μ for $\mu = 0, 1, 2, 3$ satisfy the topologically non-trivial condition (3.16b). For instance, if one (three) out of the four m_μ satisfies Eq. (3.16b), then the central charge of the edge state is 1/2 (3/2). We conclude that the gapped bulk hosts NATO. Similarly, if two (four) out of the four m_μ satisfy Eq. (3.16b), then the central charge of the edge states is 2 (4). We conclude that the gapped bulk hosts ATO.

We close this discussion by observing that the mean-field single-particle Hamiltonian (3.11c) was studied recently by Kane *et al.* in Ref. 12 [see their Eq. (58)] from a different perspective, namely that of a wire construction for paired states in the FQHE at an even-denominator filling fraction ν , say $\nu = 1/2$.

C. Integrating out the Majorana fields

In what follows, we only consider the case $v_0 \equiv v_s$, $m_0 \equiv m_s$, $v_a \equiv v_t$, and $m_a \equiv m_t$ for any $a = 1, 2, 3$. The

extension to the case of arbitrary values for v_μ and m_μ does not present major difficulties.

Integration over the Majorana fields delivers the product of two Pfaffians. There is a Pfaffian that arises from integrating over the singlet χ^0 's, and another Pfaffian that arises from integrating over the triplet χ^a 's. It follows that

$$Z \propto \int \mathcal{D}[\phi] e^{-S'}, \quad (3.17a)$$

$$S' := S_\phi + S_F, \quad (3.17b)$$

$$S_\phi := \frac{\beta L_x L_y \phi^2}{\mathfrak{a}_y 4\lambda}, \quad (3.17c)$$

$$S_F := -\frac{1}{2} \sum_{\omega, \mathbf{k}} \left[\log \left(-\omega^2 - v_s^2 k_x^2 - m_s^2 - \frac{\phi^2}{4} + m_s \phi \cos \frac{k_y}{\Lambda_y} \right) + 3 \log \left(-\omega^2 - v_t^2 k_x^2 - m_t^2 - \frac{\phi^2}{4} + m_t \phi \cos \frac{k_y}{\Lambda_y} \right) \right]. \quad (3.17d)$$

Here, we have introduced the momentum cutoff

$$\Lambda_y := \frac{1}{\mathfrak{a}_y}. \quad (3.17e)$$

The action S' controls the global symmetries of the theory. It is invariant under the global Ising-like (\mathbb{Z}_2) transformation defined by

$$\phi \mapsto -\phi \quad (3.18a)$$

if we compensate this change of sign with the change of variable

$$k_y \mapsto k_y + \pi \Lambda_y \quad (3.18b)$$

in the summation over k_y .

D. Mean-field gap equations

The saddle-point equation

$$0 \equiv \frac{\mathfrak{a}_y}{\beta L_x L_y} \frac{\partial S'}{\partial \phi} \quad (3.19)$$

are then explicitly given by

$$0 = \frac{1}{2\lambda} \phi - \frac{\mathfrak{a}_y}{\beta L_x L_y} \sum_{\omega, \mathbf{k}} \left[\frac{1}{2} \frac{\frac{1}{2} \phi - m_s \cos \frac{k_y}{\Lambda_y}}{\omega^2 + v_s^2 k_x^2 + m_s^2 + \frac{1}{4} \phi^2 - m_s \phi \cos \frac{k_y}{\Lambda_y}} + \frac{3}{2} \frac{\frac{1}{2} \phi - m_t \cos \frac{k_y}{\Lambda_y}}{\omega^2 + v_t^2 k_x^2 + m_t^2 + \frac{1}{4} \phi^2 - m_t \phi \cos \frac{k_y}{\Lambda_y}} \right]. \quad (3.20)$$

We observe that Eq. (3.20) is invariant under

$$\begin{aligned} \phi &\mapsto -\phi, \\ m_s &\mapsto -m_s, \\ m_t &\mapsto -m_t. \end{aligned} \quad (3.21)$$

It is also invariant under

$$m_s \mapsto -m_s, \quad m_t \mapsto -m_t, \quad (3.22a)$$

if we compensate this change of sign with the change of variable

$$k_y \mapsto k_y + \pi \Lambda_y \quad (3.22b)$$

in the summation over k_y . The same is true of the partition function defined in Eq. (3.17).

In the limit $\beta \rightarrow \infty$, $L_x \rightarrow \infty$, and $L_y \rightarrow \infty$ (zero temperature and thermodynamic limit), the sums become integrals in three-dimensional spacetime. Power counting predicts that those momentum integrals are logarithmically divergent in the ultraviolet. A momentum cutoff is thus needed to evaluate those integrals. It is chosen to be

$|k_x| \leq \pi \Lambda_x$ and $|k_y| \leq \pi \Lambda_y$. All integrals over the Matsubara frequencies are performed before the momentum integrals by application of the Residue theorem. To this end, the identity

$$\int_{-\infty}^{+\infty} \frac{d\omega}{2\pi} \frac{a^2}{\omega^2 + b^2} = \frac{1}{2} \frac{a^2}{\sqrt{b^2}}, \quad a, b \in \mathbb{R}, \quad (3.23)$$

is used. The remaining integral over k_x is of the form

$$\int_0^b dx \frac{1}{\sqrt{x^2 + a^2}} = \operatorname{arcsinh} \left(\frac{b}{a} \right), \quad 0 < a, b. \quad (3.24)$$

Finally, the remaining integral over k_y can be simplified by changing variable

$$q := \frac{k_y}{\Lambda_y}. \quad (3.25)$$

In summary, the saddle-point equation has become the single integral

$$0 = \frac{\phi}{2\pi\Lambda_x} - \frac{\lambda}{4\pi} \left[\frac{1}{v_s} \int_{-\pi}^{+\pi} \frac{dq}{2\pi} \left(\frac{\phi}{2\pi\Lambda_x} - \frac{2m_s}{2\pi\Lambda_x} \cos q \right) \times \operatorname{arcsinh} \left(\frac{2\pi\Lambda_x v_s}{\sqrt{4m_s^2 + \phi^2 - 4m_s \phi \cos q}} \right) \right] - \frac{3\lambda}{4\pi} [s \rightarrow t]. \quad (3.26)$$

Equation (3.26) is a non-linear equation for one unknown $\frac{\phi}{2\pi\Lambda_x}$. It can only be solved numerically for arbitrary value of λ , $\frac{m_t}{2\pi\Lambda_x}$, and $\frac{m_s}{2\pi\Lambda_x}$ (set $v_s = v_t \equiv 1$) if no further approximation is imposed. Nevertheless, it is still useful to look at two limiting cases of the saddle-point equation (3.26).

Case $\lambda = 0$. The solution for ϕ is simply

$$\phi = 0. \quad (3.27)$$

Case $m_s = m_t = 0$. Assuming $\phi \neq 0$, Eq. (3.26) simplifies to (set $v_s = v_t \equiv 1$)

$$1 = \frac{\lambda}{\pi} \operatorname{arcsinh} \left(\frac{2\pi\Lambda_x}{|\phi|} \right). \quad (3.28)$$

Since $\operatorname{arcsinh} \left(\frac{2\pi\Lambda_x}{|\phi|} \right)$ is positive, we must require $\lambda >$

0 to find the solution of ϕ from (3.28). Non-vanishing solutions for ϕ are

$$|\phi| = 2\pi\Lambda_x \frac{1}{\sinh \left(\frac{\pi}{\lambda} \right)}, \quad \lambda > 0. \quad (3.29)$$

E. Approximate mean-field gap equations

Insertion of the asymptotic expansion

$$\operatorname{arcsinh}(x) \approx \ln(2x) + \mathcal{O}(x^{-2}) \quad (3.30)$$

into the saddle-point equation (3.26) gives

$$0 = \frac{\phi}{2\pi\Lambda_x} - \frac{\lambda}{4\pi} \left[\frac{1}{v_s} \int_{-\pi}^{+\pi} \frac{dq}{2\pi} \left(\frac{\phi}{2\pi\Lambda_x} - \frac{2m_s}{2\pi\Lambda_x} \cos q \right) \times \ln \left(\frac{4\pi\Lambda_x v_s}{\sqrt{4m_s^2 + \phi^2 - 4m_s \phi \cos q}} \right) \right] - \frac{3\lambda}{4\pi} [s \rightarrow t] \quad (3.31a)$$

with the conditions

$$0 \leq \sqrt{4m_s^2 + \phi^2 - 4m_s \phi \cos q} \ll 2\pi\Lambda_x v_s \quad (3.31b)$$

and

$$0 \leq \sqrt{4m_t^2 + \phi^2 - 4m_t \phi \cos q} \ll 2\pi\Lambda_x v_t. \quad (3.31c)$$

The integrals in Eq. (3.31a) can be carried out. There follows

$$0 = \frac{\phi}{2\pi\Lambda_x} - \frac{\lambda}{4\pi} \frac{1}{v_s} \left\{ \frac{\phi}{2\pi\Lambda_x} \times \ln \left(\frac{4\sqrt{2}\pi\Lambda_x v_s}{\sqrt{4m_s^2 + \phi^2 + |4m_s^2 - \phi^2|}} \right) - \frac{1}{4} \left(\frac{\phi}{2\pi\Lambda_x} \right)^{-1} \left[\left(\frac{\phi}{2\pi\Lambda_x} \right)^2 + \left(\frac{2m_s}{2\pi\Lambda_x} \right)^2 - \left| \left(\frac{\phi}{2\pi\Lambda_x} \right)^2 - \left(\frac{2m_s}{2\pi\Lambda_x} \right)^2 \right| \right] \right\} - \frac{3\lambda}{4\pi} \frac{1}{v_t} \{s \rightarrow t\} \quad (3.32a)$$

with the conditions

$$0 \leq 2|m_s| + |\phi| \ll 2\pi\Lambda_x v_s \quad (3.32b)$$

and

$$0 \leq 2|m_t| + |\phi| \ll 2\pi\Lambda_x v_t. \quad (3.32c)$$

From now on, we treat the case $m_s = 0$ for which

$$\begin{aligned}
0 = & \frac{\phi}{2\pi\Lambda_x} - \frac{\lambda}{4\pi} \frac{1}{v_s} \frac{\phi}{2\pi\Lambda_x} \times \ln \left(\frac{4\pi\Lambda_x v_s}{|\phi|} \right) \\
& - \frac{3\lambda}{4\pi} \frac{1}{v_t} \left\{ \frac{\phi}{2\pi\Lambda_x} \times \ln \left(\frac{4\sqrt{2}\pi\Lambda_x v_t}{\sqrt{4m_t^2 + \phi^2 + |4m_t^2 - \phi^2|}} \right) \right. \\
& \left. - \frac{1}{4} \left(\frac{\phi}{2\pi\Lambda_x} \right)^{-1} \left[\left(\frac{\phi}{2\pi\Lambda_x} \right)^2 + \left(\frac{2m_t}{2\pi\Lambda_x} \right)^2 - \left| \left(\frac{\phi}{2\pi\Lambda_x} \right)^2 - \left(\frac{2m_t}{2\pi\Lambda_x} \right)^2 \right| \right] \right\}
\end{aligned} \tag{3.33a}$$

with the conditions

$$0 \leq |\phi| \ll 2\pi\Lambda_x v_s \tag{3.33b}$$

and

$$0 \leq 2|m_t| + |\phi| \ll 2\pi\Lambda_x v_t. \tag{3.33c}$$

Equation (3.33) is solved for the following four cases.

Case $m_t = 0$. Assuming $\phi \neq 0$, Eq. (3.33) simplifies to (set $v_s = v_t \equiv 1$)

$$1 = \frac{\lambda}{\pi} \ln \left(\frac{4\pi\Lambda_x}{|\phi|} \right) \tag{3.34a}$$

with

$$0 \leq |\phi| \ll 2\pi\Lambda_x. \tag{3.34b}$$

Since $\ln(x)$ is positive for $x > 1$, we must require $\lambda > 0$ to find the solution of ϕ from (3.34a). Hence, a solution with a non-vanishing $|\phi|/(2\pi\Lambda_x)$ is

$$\frac{|\phi|}{2\pi\Lambda_x} = 2 \times e^{-\frac{\pi}{\lambda}}, \quad \lambda > 0. \tag{3.35}$$

This is the usual weak-coupling BCS gap.

Case $|\phi| < 2|m_t|$. It follows that $4m_t^2 - \phi^2 > 0$. Assuming $\phi \neq 0$, Eq. (3.33) simplifies to (set $v_s = v_t \equiv 1$)

$$1 = \frac{\lambda}{4\pi} \ln \left(\frac{4\pi\Lambda_x}{|\phi|} \right) + \frac{3\lambda}{4\pi} \ln \left(\frac{2\pi\Lambda_x}{|m_t|} \right) - \frac{3\lambda}{8\pi} \tag{3.36a}$$

with

$$0 \leq |\phi| \ll 2\pi\Lambda_x \tag{3.36b}$$

and

$$0 \leq 2|m_t| + |\phi| \ll 2\pi\Lambda_x. \tag{3.36c}$$

Hence, a solution with a non-vanishing $|\phi|/(2\pi\Lambda_x)$ is

$$\frac{|\phi|}{2\pi\Lambda_x} = 2 \times e^{-3/2} \times \left(\frac{|m_t|}{2\pi\Lambda_x} \right)^{-3} \times e^{-4\pi/\lambda}. \tag{3.37}$$

Increasing $|m_t|$ decreases $|\phi|$. Increasing $\lambda > 0$ decreases $|\phi|$. There is a competition between $\lambda > 0$ and $|m_t|$.

Case $|\phi| > 2|m_t|$. It follows that $4m_t^2 - \phi^2 < 0$. Assuming $\phi \neq 0$, Eq. (3.33) simplifies to (set $v_s = v_t \equiv 1$)

$$1 = \frac{\lambda}{\pi} \ln \left(\frac{4\pi\Lambda_x}{|\phi|} \right) - \frac{3\lambda}{2\pi} \left(\frac{m_t}{\phi} \right)^2 \tag{3.38a}$$

with

$$0 \leq |\phi| \ll 2\pi\Lambda_x \tag{3.38b}$$

and

$$0 \leq 2|m_t| + |\phi| \ll 2\pi\Lambda_x. \tag{3.38c}$$

Hence, a solution with a non-vanishing $|\phi|/(2\pi\Lambda_x)$ is

$$\frac{|\phi|}{2\pi\Lambda_x} e^{+\frac{3}{2} \left(\frac{m_t}{\phi} \right)^2} = 2 e^{-\pi/\lambda}. \tag{3.39}$$

Case $\phi = \pm 2m_t$. Assuming $\phi \neq 0$, Eq. (3.33) simplifies to (set $v_s = v_t \equiv 1$)

$$1 = \frac{\lambda}{\pi} \ln \left(\frac{4\pi\Lambda_x}{|\phi|} \right) - \frac{3\lambda}{8\pi} \tag{3.40a}$$

with

$$0 \leq 2|\phi| \ll 2\pi\Lambda_x. \tag{3.40b}$$

Hence, a solution with a non-vanishing $|\phi|/(2\pi\Lambda_x)$ is

$$\frac{|\phi|}{2\pi\Lambda_x} = \frac{2|m_t|}{2\pi\Lambda_x} = 2 \times e^{-3/8} \times e^{-\frac{\pi}{\lambda}}. \tag{3.41}$$

F. Hessian at the saddle points

We are going to compute the Hessian of the effective potential defined by S' in Eq. (3.17). To this end, define

$$V_{\text{eff}} := \frac{\mathbf{a}_y}{\beta L_x L_y} S'. \tag{3.42}$$

We begin with the saddle points of V_{eff} for $m_s = 0$ within logarithmic accuracy. They are simply given by the right-hand side of Eq. (3.33a). Next, we turn our attention to the second-order derivative of V_{eff} ,

$$\begin{aligned} \frac{\partial^2 V_{\text{eff}}}{\partial \phi^2} = & \frac{1}{2\lambda} - \frac{1}{8\pi} \frac{1}{v_s} \left[\ln \left(\frac{4\pi\Lambda_x v_s}{|\phi|} \right) - 1 \right] \\ & - \frac{3}{8\pi} \frac{1}{v_t} \left\{ \ln \left(\frac{4\sqrt{2}\pi\Lambda_x v_t}{\sqrt{4m_t^2 + \phi^2 + |4m_t^2 - \phi^2|}} \right) - 1 \right. \\ & \left. + \frac{1}{4} \left(\frac{\phi}{2\pi\Lambda_x} \right)^{-2} \left[\left(\frac{\phi}{2\pi\Lambda_x} \right)^2 + \left(\frac{2m_t}{2\pi\Lambda_x} \right)^2 - \left| \left(\frac{\phi}{2\pi\Lambda_x} \right)^2 - \left(\frac{2m_t}{2\pi\Lambda_x} \right)^2 \right| \right] \right\} \end{aligned} \quad (3.43a)$$

with

$$0 \leq |\phi| \ll 2\pi\Lambda_x v_s \quad (3.43b)$$

and

$$0 \leq 2|m_t| + |\phi| \ll 2\pi\Lambda_x v_t. \quad (3.43c)$$

There are four cases to consider.

Case $m_t = 0$. Insertion of Eq. (3.35) into Eq. (3.43) gives (set $v_s = v_t \equiv 1$)

$$\left. \frac{\partial^2 V_{\text{eff}}}{\partial \phi^2} \right|_{\text{saddle}} = \frac{1}{2\pi} > 0. \quad (3.44)$$

Solution (3.35) is a local minima of the effective potential.

Case $|\phi| < 2|m_t|$. Insertion of Eq. (3.37) into Eq. (3.43) gives (set $v_s = v_t \equiv 1$)

$$\left. \frac{\partial^2 V_{\text{eff}}}{\partial \phi^2} \right|_{\text{saddle}} = \frac{1}{8\pi} > 0. \quad (3.45)$$

Solution (3.37) is a local minima of the effective potential.

Case $|\phi| > 2|m_t|$. Insertion of Eq. (3.39) into Eq. (3.43) gives (set $v_s = v_t \equiv 1$)

$$\left. \frac{\partial^2 V_{\text{eff}}}{\partial \phi^2} \right|_{\text{saddle}} = \frac{1}{2\pi} - \frac{3}{2\pi} \left(\frac{m_t}{\phi} \right)^2 > 0. \quad (3.46)$$

Solution (3.39) is a local minima of the effective potential.

Case $\phi = \pm 2m_t$. Insertion of Eq. (3.41) into Eq. (3.43) gives (set $v_s = v_t \equiv 1$)

$$\left. \frac{\partial^2 V_{\text{eff}}}{\partial \phi^2} \right|_{\text{saddle}} = \frac{1}{8\pi} > 0. \quad (3.47)$$

Solution (3.41) with $\lambda > 0$ is a local minima of the effective potential.

G. Interpretation

To proceed, we recall the definition of the mean-field Majorana gap (3.15)

$$\Delta_0 \equiv \Delta_s := \frac{|\phi|}{2} \quad (3.48a)$$

for the singlet Majorana field with $m_s = 0$, and

$$\Delta_a \equiv \Delta_t := \left| m_t - \frac{|\phi|}{2} \right|, \quad a = 1, 2, 3 \quad (3.48b)$$

for the triplet of Majorana fields, and the corresponding topological criteria (3.16). One observes that the singlet Majorana gap Δ_s (3.48a) is non-vanishing as long as $\phi \neq 0$.

The approximate mean-field solution given by Eqs. (3.35), (3.37), (3.39), and (3.41) when $|m_t| = 0$, $|\phi| < 2|m_t|$, $|\phi| > 2|m_t|$, and $|\phi| = 2|m_t|$, respectively, imply the mean-field phase diagram shown in Fig. 5. More specifically, we first look at the line $m_t = 0$, along which we have a non-vanishing value of ϕ . This corresponds to a phase with (mean-field) ATO, for which the boundary realizes a CFT with central charge 2 as both the singlet and triplet of chiral Majorana edge states are gapless. We also find that $|\phi|$ reaches its maximum value when $m_t = 0$ for a given $\lambda > 0$. The generic trend is that $|\phi|$ decreases as $|m_t|$ increases. If we increase $|m_t|$ a little away from 0, $|\phi|$ decreases a little. However, the ATO phase is robust, for the mean-field bulk gap Δ_s and Δ_t (3.48) remain non-vanishing. We have to increase $|m_t|$ until it satisfies $2|m_t| = |\phi|$ for the mean-field triplet bulk gap Δ_t (3.48b) to close. Only then can the (mean-field) ATO phase be destroyed. The triplet bulk gap Δ_t reopens when $2|m_t| > |\phi|$, however the triplet of chiral Majorana edge states are now gapped, leaving only a singlet of massless chiral Majorana edge states. This mean-field phase supports (mean-field) NATO, for which the boundary realizes a CFT with central charge 1/2. In the large $|m_t|$ limit, the value of $|\phi|$ is further suppressed [see Eq. (3.37)]. However, the mean-field bulk gap Δ_s and Δ_t remain gapped, whatever the small but non-vanishing value of $|\phi|$ is.

The assumption that the singlet mass m_s vanishes in order to derive the non-vanishing solutions (3.35), (3.37), (3.39), and (3.41) to the gap equation (3.33) is not essential as long as a non-vanishing m_s is smaller in magnitude than the saddle-point $|\phi/2|$. This is to say that the ATO and NATO phases for $\lambda > 0$ and $m_s=0$ extend to non-vanishing yet not too strong $|\phi/2| > |m_s| > 0$. The ATO and NATO phases do not require a precise tuning of the two-leg ladders to their Ising critical point provided the detuning is smaller in magnitude than $|\phi/2|$.

IV. BEYOND MEAN-FIELD THEORY: DIMENSIONAL CROSSOVER FROM A RANDOM PHASE APPROXIMATION

The mean-field approximation of Sec. III is done in two-dimensional space. It posits that all excitations belong to a quartet of point-like particles obeying the Majorana equal-time algebra. However, the line $m_t = m_s = 0$ when $v_\mu = v$ for $\mu = 0, 1, 2, 3$ in Fig. 3 corresponds to an integrable model for which this is not the case. As was alluded to below Eq. (2.5), Hamiltonian (2.5) with $\lambda > 0$ is a massive theory in which the quartet of Majoranas do not exist as sharp (coherent) excitations, i.e., none of the components

$$G_{\mu, M, m; \mu' M', m'}^{1d}(\omega, k_x) := - \langle 0 | \widehat{\chi}_{M, m}^\mu(\omega, k_x) \widehat{\chi}_{M', m'}^{\mu'}(-\omega, -k_x) | 0 \rangle \quad (4.1)$$

(the ket $|0\rangle$ denotes the ground state) support poles. Here, ω is a fermionic Matsubara frequency, k_x is a one-dimensional momentum, $\mu, \mu' = 0, 1, 2, 3$ refer to the index for the quartet of Majorana fields, $M, M' = L, R$ refer to the left- and right-moving components of the Majorana fields, and $m, m' = 1, \dots, n$ refer to the index of the ladders.

The line $m_t = m_s = 0$ when $v_\mu = v$ for $\mu = 0, 1, 2, 3$ in Fig. 3 consists of decoupled one-dimensional Gross-Neveu Hamiltonians with $O(4)$ symmetry, recall Eq. (2.5d), each one of which has the Lagrangian density

$$\widehat{\mathcal{L}}_{\text{GN}} := \widehat{\mathcal{L}}_0 + \widehat{\mathcal{H}}_{\text{int}}, \quad (4.2a)$$

$$\widehat{\mathcal{L}}_0 = \frac{1}{2} \sum_{\mu=0}^3 [\widehat{\chi}_L^\mu (\partial_\tau + iv \partial_x) \widehat{\chi}_L^\mu + \widehat{\chi}_R^\mu (\partial_\tau - iv \partial_x) \widehat{\chi}_R^\mu], \quad (4.2b)$$

$$\widehat{\mathcal{H}}_{\text{int}} = \frac{\lambda}{4} \left(\sum_{\mu=0}^3 \widehat{\chi}_L^\mu \widehat{\chi}_R^\mu \right)^2. \quad (4.2c)$$

where the velocity v and the coupling λ are all real valued.

We are going to extract the single-particle Green function for the Majorana fermions with the Hamiltonian (4.2) using non-perturbative results valid for integrable systems. We will then treat a non-vanishing mass $m_t \neq 0$ non-perturbatively within a Random Phase Approximation (RPA).

It is known²⁰ that the $O(4)$ GN defined by the Lagrangian density (4.2) is equivalent to two independent copies of the sine-Gordon model. We identify the first copy as the spin-sector and the second copy as the charge sector for interacting spin-1/2 electrons. In turn, the creation $\widehat{\psi}_{M, \sigma}^\dagger$ and annihilation $\widehat{\psi}_{M, \sigma}$ operators for the elec-

trons are related to the Majorana fermions by

$$\widehat{\psi}_{M, \uparrow}^\dagger \equiv \frac{1}{\sqrt{2}} (\widehat{\chi}_M^1 - i \widehat{\chi}_M^2), \quad \widehat{\psi}_{M, \uparrow} \equiv \frac{1}{\sqrt{2}} (\widehat{\chi}_M^1 + i \widehat{\chi}_M^2), \quad (4.3a)$$

$$\widehat{\psi}_{M, \downarrow}^\dagger \equiv \frac{1}{\sqrt{2}} (\widehat{\chi}_M^3 - i \widehat{\chi}_M^0), \quad \widehat{\psi}_{M, \downarrow} \equiv \frac{1}{\sqrt{2}} (\widehat{\chi}_M^3 + i \widehat{\chi}_M^0), \quad (4.3b)$$

where $M = L, R$ and $\sigma = \uparrow, \downarrow$. By relying on Abelian bosonization rules, the $O(4)$ GN Lagrangian density (4.2) becomes

$$\widehat{\mathcal{L}}_{\text{GN}} = \widehat{\mathcal{L}}_{\text{GN}, s} + \widehat{\mathcal{L}}_{\text{GN}, c}, \quad (4.4a)$$

$$\widehat{\mathcal{L}}_{\text{GN}, s} = \frac{1}{2} \left[v_s^{-1} (\partial_\tau \widehat{\varphi}_s)^2 + v_s (\partial_x \widehat{\varphi}_s)^2 \right] - \frac{\lambda}{4} \cos(\beta \widehat{\varphi}_s), \quad (4.4b)$$

$$\widehat{\mathcal{L}}_{\text{GN}, c} = \frac{1}{2} \left[v_c^{-1} (\partial_\tau \widehat{\varphi}_c)^2 + v_c (\partial_x \widehat{\varphi}_c)^2 \right] - \frac{\lambda}{4} \cos(\beta \widehat{\varphi}_c), \quad (4.4c)$$

with

$$v_s = v_c \equiv v \quad (4.4d)$$

and

$$\beta = \sqrt{\frac{8\pi}{1 + \frac{\lambda}{2\pi}}}. \quad (4.4e)$$

Equation (4.4) is also derived in Sec. VII starting from the spin-1/2 lattice model depicted in Fig. 2.

The quantum critical point $\lambda = 0$ ($\beta^2 = 8\pi$) supports an $\widehat{su}(2)_1 \oplus \widehat{su}(2)_1$ current algebra. When $\lambda > 0$ ($\beta^2 < 8\pi$) each cosine interaction becomes marginally relevant, a spectral gap opens up, and soliton-like excitations (kinks) by which the asymptotic expectation values of $\widehat{\varphi}_a(x, \tau)$ with $a = s, c$ at $x = -\infty$ and $x = +\infty$ changes by $\pm 2\pi/\beta$ over a region of size $1/M$ can be thought of as massive particles with the mass M a function of the deviation $8\pi - \beta^2 > 0$. At $\beta^2 = 4\pi$, $\widehat{\mathcal{L}}_{\text{GN}, a}$ is a non-interacting massive Dirac theory for both $a = s$ and $a = c$. When $\beta^2 < 4\pi$, breather modes supplement the kinks as massive point-like excitations.

If the real-valued scalar field $\widehat{\varphi}_a(\tau, x)$ is decomposed into left- and right-moving parts according to the rule

$$\widehat{\varphi}_a(\tau, x) = \widehat{\varphi}_{a, R}(\tau + ix) + \widehat{\varphi}_{a, L}(\tau - ix), \quad (4.5a)$$

it is then possible to use the Mandelstam representation

$$\widehat{\psi}_{M, \sigma} := \frac{\eta_\sigma}{\sqrt{2\pi}} e^{i\sqrt{2\pi} \widehat{\varphi}_{c, M}} e^{if_\sigma \sqrt{2\pi} \widehat{\varphi}_{s, M}} \quad (4.5b)$$

with $M = L, R$, $\sigma = \uparrow, \downarrow$, $f_\uparrow = -f_\downarrow = 1$, and η_σ the Klein factors fulfilling

$$\{\eta_\sigma, \eta_{\sigma'}\} = 2\delta_{\sigma, \sigma'}. \quad (4.5c)$$

The chiral vertex operator $\exp(\pm i\sqrt{2\pi}\widehat{\varphi}_{a,M})$ carries the Lorentz spin

$$s := \pm 1/4, \quad (4.6)$$

i.e., under the rotation

$$\tau + ix \mapsto e^{i\alpha}(\tau + ix) \quad (4.7)$$

of two-dimensional Euclidean space, it is multiplied by the phase $\exp(\pm i\alpha/4)$. The chiral electron annihilation operator, which must carry the Lorentz spin $s = 1/2$, is glued by taking the product of two chiral vertex operators, each of which carries the Lorentz spin $s = 1/4$, according to Eq. (4.5).

To calculate the two-point correlation functions for the chiral Majorana fields, they are first expressed in terms of two-point functions for the chiral electron fields using Eq. (4.3). The Mandelstam representation (4.5) is then used to represent the two-point Green's functions for the Majorana fields in terms of two-point functions for the chiral vertex operators. Finally, the two-point functions for the chiral vertex operators are calculated using the form factors of the massive integrable theory defined by the Lagrangian density (4.4).

In a relativistically invariant massive integrable theory in two-dimensional Euclidean space, all multiparticle states are the kets

$$|\theta_n, \dots, \theta_1\rangle_{\epsilon_n, \dots, \epsilon_1} \quad (4.8a)$$

with the many-body energy

$$\sum_{j=1}^n E_{\epsilon_j}(\theta_j), \quad E_{\epsilon_j}(\theta_j) := M \cosh \theta_j, \quad (4.8b)$$

the many-body momentum

$$\sum_{j=1}^n P_{\epsilon_j}(\theta_j), \quad P_{\epsilon_j}(\theta_j) := \frac{M}{v} \sinh \theta_j, \quad (4.8c)$$

where θ_i denotes the rapidity of a single-particle state with the quantum number ϵ_i . They are pairwise orthogonal and orthogonal to the ground state $|0\rangle$ with the resolution of the identity

$$1 = |0\rangle\langle 0| + \sum_{n=1}^{+\infty} \sum_{\epsilon_i} \int_{-\infty}^{+\infty} \frac{d\theta_1 \dots d\theta_n}{(2\pi)^n n!} \times |\theta_n, \dots, \theta_1\rangle_{\epsilon_n, \dots, \epsilon_1} \langle \theta_1, \dots, \theta_n|. \quad (4.8d)$$

The two-point functions for the chiral vertex operators are calculated using an integral representation for the form factor

$$\langle 0 | e^{\pm i\sqrt{2\pi}\widehat{\varphi}_{a,M}} | \theta_n, \dots, \theta_1 \rangle_{\epsilon_n, \dots, \epsilon_1} \quad (4.9)$$

due to Ref. 21. Following Refs. 22 and 23 we will truncate the resolution of the identity (4.8d) to the order $n = 1$ when evaluating the form factors for the electron operators.

The one-particle form factors for the pair of chiral vertex operators $\exp(i\sqrt{2\pi}\widehat{\varphi}_{a,M})$ between the vacuum and a state supporting a single soliton are

$$\langle 0 | e^{i\sqrt{2\pi}\widehat{\varphi}_{a,R}} | \theta \rangle \approx \sqrt{Z_0} (2\pi M v^{-1})^{1/4} e^{+\theta/4}, \quad (4.10a)$$

$$\langle 0 | e^{i\sqrt{2\pi}\widehat{\varphi}_{a,L}} | \theta \rangle \approx \sqrt{Z_0} (2\pi M v^{-1})^{1/4} e^{-\theta/4}. \quad (4.10b)$$

The dependence on the rapidity θ is fixed by Lorentz invariance, whereas the positive constant Z_0 is not fixed by symmetry, but was calculated in Ref. 21 to be

$$Z_0 \approx 0.92. \quad (4.10c)$$

In the same work it was demonstrated that most of the spectral weight is contained in the emission of a single kink. For example, about 80 percent of the spectral weight in the spectral functions entering the Majorana two-point functions (4.12) originate from the emission of a single kink. After substituting these matrix elements into the Lehmann expansion for the Majorana two-point functions in (1+1)-dimensional Euclidean space, we obtain, for any $\mu = 0, 1, 2, 3$ and after setting $v = 1$,

$$G_{\text{LL}}^{\text{1d}}(\tau, x) := -\langle 0 | \widehat{\chi}_{\text{L}}^{\mu}(\tau, x) \widehat{\chi}_{\text{L}}^{\mu}(0, 0) | 0 \rangle = -Z_0^2 \left(\frac{\tau + ix}{\tau - ix} \right)^{1/2} \left[\int_{-\infty}^{+\infty} \frac{d\theta}{2\pi} e^{-\theta/2} e^{-M\rho \cosh \theta} \right]^2 = -\frac{Z_0^2 e^{-2M\rho}}{2\pi(\tau - ix)}, \quad (4.11a)$$

$$G_{\text{RR}}^{\text{1d}}(\tau, x) := -\langle 0 | \widehat{\chi}_{\text{R}}^{\mu}(\tau, x) \widehat{\chi}_{\text{R}}^{\mu}(0, 0) | 0 \rangle = -Z_0^2 \left(\frac{\tau - ix}{\tau + ix} \right)^{1/2} \left[\int_{-\infty}^{+\infty} \frac{d\theta}{2\pi} e^{+\theta/2} e^{-M\rho \cosh \theta} \right]^2 = -\frac{Z_0^2 e^{-2M\rho}}{2\pi(\tau + ix)}, \quad (4.11b)$$

$$G_{\text{LR}}^{\text{1d}}(\tau, x) = G_{\text{RL}}^{\text{1d}}(\tau, x) := -\langle 0 | \widehat{\chi}_{\text{L}}^{\mu}(\tau, x) \widehat{\chi}_{\text{R}}^{\mu}(0, 0) | 0 \rangle = -Z_0^2 M \left[\int_{-\infty}^{+\infty} \frac{d\theta}{2\pi} e^{-M\rho \cosh \theta} \right]^2 = -\frac{Z_0^2 M K_0^2(M\rho)}{\pi^2}, \quad (4.11c)$$

where

$$K_0(z) := \frac{1}{2} \int_{-\infty}^{+\infty} dt e^{-z \cosh z}, \quad \rho := \sqrt{\tau^2 + x^2}. \quad (4.11d)$$

Fourier transformation to imaginary frequency ($\bar{\omega}$) and momentum (q) space followed by the analytic continuation $\bar{\omega} \rightarrow -i\omega + 0^+$ delivers the retarded two-point Green functions for the chiral Majorana fields given by

$$G_{\text{LL}}^{\text{1d}}(\omega, q) := \lim_{\bar{\omega} \rightarrow -i\omega + 0^+} \int d\tau dx e^{i\bar{\omega}\tau - iqx} G_{\text{LL}}^{\text{1d}}(\tau, x) \approx \frac{Z_0^2}{\omega - q} \left(1 - \frac{1}{\sqrt{1 - s^2/(2M)^2}} \right), \quad (4.12a)$$

$$G_{\text{RR}}^{\text{1d}}(\omega, q) := \lim_{\bar{\omega} \rightarrow -i\omega + 0^+} \int d\tau dx e^{i\bar{\omega}\tau - iqx} G_{\text{RR}}^{\text{1d}}(\tau, x) \approx \frac{Z_0^2}{\omega + q} \left(1 - \frac{1}{\sqrt{1 - s^2/(2M)^2}} \right), \quad (4.12b)$$

$$G_{\text{LR}}^{\text{1d}}(\omega, q) = G_{\text{RL}}^{\text{1d}}(\omega, q) := \lim_{\bar{\omega} \rightarrow -i\omega + 0^+} \int d\tau dx e^{i\bar{\omega}\tau - iqx} G_{\text{LR}}^{\text{1d}}(\tau, x) \approx -\frac{Z_0^2}{2M} \frac{2}{\pi} \frac{\arcsin(s/2M)}{[s/(2M)] \sqrt{1 - [s/(2M)]^2}}, \quad (4.12c)$$

where

$$s^2 := \omega^2 - q^2. \quad (4.12d)$$

Observe that the Green functions (4.12a) and (4.12b) are even functions of M , while the Green function (4.12c) is an odd function of M . This latter fact follows from the bond operator (2.7) being odd under any transformation (2.6) with $\sigma_{\text{L},m} \sigma_{\text{R},m+1} = -1$.

Once we turn on a non-vanishing m_t , we restore true two-dimensionality of space. In the spirit of the RPA for dimensional crossovers from lower to higher dimensions, we make the RPA Ansatz for the retarded Green's function in momentum space

$$\widehat{G}^{\text{2d RPA}}(\omega, k_x, k_y) := \frac{1}{\left[\widehat{G}^{\text{1d}}(\omega, k_x) \right]^{-1} - \widehat{M}(k_y)}, \quad (4.13a)$$

where

$$\widehat{G}^{\text{1d}}(\omega, k_x) := \begin{pmatrix} G_{\text{LL}}^{\text{1d}}(\omega, k_x) & G_{\text{LR}}^{\text{1d}}(\omega, k_x) \\ G_{\text{RL}}^{\text{1d}}(\omega, k_x) & G_{\text{RR}}^{\text{1d}}(\omega, k_x) \end{pmatrix} \quad (4.13b)$$

and the Fourier transform of the perturbation $\widehat{M}(k_y)$ given by

$$\widehat{M}(k_y) := \begin{pmatrix} 0 & m_\mu e^{+ik_y} \\ m_\mu e^{-ik_y} & 0 \end{pmatrix}. \quad (4.13c)$$

If the operator-valued denominator on the right-hand side of Eq. (4.13a) acquires first-order zeros as eigenvalues, then this RPA predicts that a non-vanishing m_μ turns the Majorana fields into well-defined quasiparticles. The condition for this to happen is that the determinant of the denominator on the right-hand side of Eq. (4.13a) vanishes, namely

$$0 = 1 - 2m_\mu G_{\text{LR}}^{\text{1d}}(\omega, k_x) \cos k_y - m_\mu^2 \det \widehat{G}^{\text{1d}}(\omega, k_x). \quad (4.14)$$

Substituting the retarded Green's functions from Eq. (4.12), we obtain the dispersion for the triplet of Majoranas (the singlet ones at $m_s = 0$ do not propagate, at least in this RPA formalism) from solving

$$\cos k_y \approx \frac{1 - \left(\frac{Z_0^2 m_t}{2M} \right)^2 \left[g^2 \left(\frac{s}{2M} \right) - f^2 \left(\frac{s}{2M} \right) \right]}{(-2) \left(\frac{Z_0^2 m_t}{2M} \right) f \left(\frac{s}{2M} \right)}, \quad (4.15a)$$

where we have introduced the auxiliary functions

$$g(x) := \frac{1}{x} \left(1 - \frac{1}{\sqrt{1 - x^2}} \right), \quad f(x) := \frac{2}{\pi} \frac{\arcsin(x)}{x \sqrt{1 - x^2}}, \quad (4.15b)$$

with the limiting values

$$\lim_{x \rightarrow 0} g(x) = 0, \quad \lim_{x \rightarrow 0} f(x) = 2/\pi, \quad (4.15c)$$

and the asymptotic expansion for $|x| \ll 1$

$$g(x) = -\frac{1}{2}x - \frac{3}{8}x^3 \dots, \quad f(x) = \frac{2}{\pi} \left(1 + \frac{2}{3}x^2 + \dots \right). \quad (4.15d)$$

We note that the RPA spectrum (4.15a) is invariant under the simultaneous transformation

$$k_y \mapsto k_y \pm \pi, \quad m_t \mapsto -m_t. \quad (4.16)$$

For small $|m_t/M| \ll 1$, we deduce from Eq. (4.15) the relation

$$(s/2M)^2 \approx 1 - (Z_0^2 m_t/M)^2 \cos^2 k_y, \quad |k_y| < \pi/2. \quad (4.17)$$

As it should be, no RPA excitations can be found below the threshold $2M$ for the two-soliton continuum when

$m_t = 0$. However, for any infinitesimal $m_t \neq 0$, one finds RPA excitations that are dispersing along the m direction with the momentum k_y below the threshold $2M$.

For arbitrary $|m_t/M|$, one can solve Eq. (4.15) numerically, thereby confirming the analytical results obtained for $|m_t/M| \ll 1$. Figure 7 displays the values of the pair

$$(k_y, s) \equiv (k_y, \sqrt{\omega^2 - k_x^2}) \quad (4.18)$$

that solve Eq. (4.15a) holding

$$A := -\frac{Z_0^2 m_t}{2M} > 0 \quad (4.19)$$

fixed. By inspection of the dispersions (s, k_y) for different values of A , we deduce the existence of a spectral gap except for the special case when

$$A \rightarrow \frac{\pi}{2}, \quad (4.20)$$

which is nothing but the solution to Eq. (4.15a) in the limit $k_y \rightarrow 0$ and $s \rightarrow 0$, namely the solution to

$$0 = \left(1 - \frac{2}{\pi} A\right)^2. \quad (4.21)$$

The condition

$$-\frac{Z_0^2 m_t}{2M} = \frac{\pi}{2} \quad (4.22)$$

is nothing but the RPA counterpart to the mean-field transition from the ATO to the NATO phases by which the number of Majorana edge states changes. The numerical value of the condition (4.22) with $Z_0^2 \approx 0.85$ is

$$\frac{|m_t|}{M} \approx 3.7. \quad (4.23)$$

When $|A - (\pi/2)| \ll 1$, we can expand the right-hand side of Eq. (4.15a) in powers of $s/(2M)$ with the help of the asymptotic expansion (4.15d). One finds the dispersion

$$\begin{aligned} \omega^2 \approx k_x^2 + \left[\frac{32}{3\pi A} \cos k_y + \left(1 - \frac{64}{3\pi^2}\right) \right]^{-1} \left(\frac{4M}{A}\right)^2 \\ \times \left[\sin^2 k_y + \left(\frac{2A}{\pi} - \cos k_y\right)^2 \right]. \end{aligned} \quad (4.24a)$$

The squared mass [take $A \approx \pi/2$ in the first square bracket and $k_x = k_y = 0$ on the right-hand-side of Eq. (4.24a)]

$$m_{\text{RPA}}^2 \approx \left(\frac{8M}{\pi A}\right)^2 \left(A - \frac{\pi}{2}\right)^2 \ll M^2 \quad (4.24b)$$

for the triplet of Majorana fields follows.

At values of $A > \pi/2$ the gap increases fast. It should also be noted that the dispersion does not include the entire Brillouin zone; there is a critical value of k_y beyond which it crosses into the two-soliton continuum above the energy threshold $2M$.

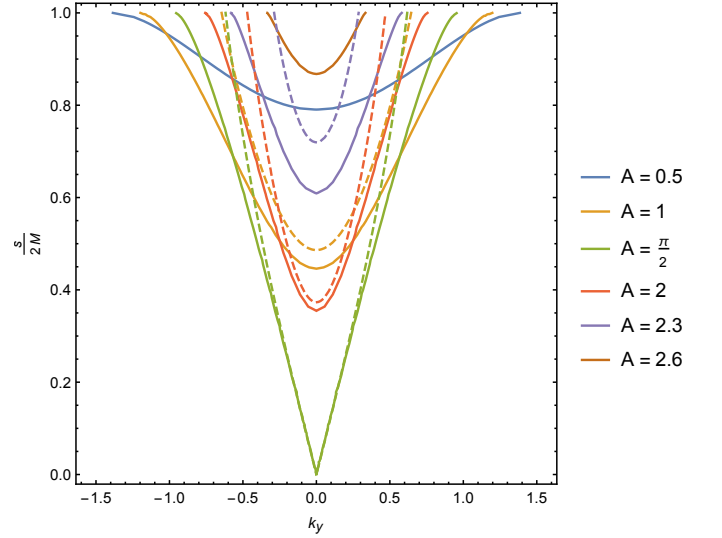


FIG. 7. (Color online) The solid lines are the dispersions $s/(2M)$ for the triplet of Majorana modes as a function of k_y that follows from solving Eq. (4.15a) for different values of $A = -Z_0^2 m_t/(2M)$. The dashed lines are the corresponding dispersions obtained from the approximate dispersion relation (4.24a).

V. TWO-DIMENSIONAL MAJORANA FERMIONS, ONE-DIMENSIONAL SOLITONS

Both the mean-field approach and the one based on combining the exact solution for the Majorana two-point correlation functions of the one-dimensional Gross-Neveu Hamiltonian (2.5) with the RPA tell us that the excitations of the model of coupled wires obeying periodic boundary conditions in all space directions can include Majorana modes.

In the limit $m_t = m_s = 0$, the low lying excitations of the Gross-Neveu Hamiltonian (2.5) are exclusively made of solitons. These solitons propagate along the x direction only (i.e., in one dimension only) above the energy threshold M introduced in Sec. IV. Remarkably, these solitons are also present in the spectrum when a small in magnitude $m_t \neq 0$ is added to the Gross-Neveu Hamiltonian (2.5), i.e., they are not confined by the crossover to two-dimensional space induced by the coupling $m_t \neq 0$. To arrive at this conclusion, we proceed as follows.

We are going to show that the symmetry (3.5), which implies the conservation of the m -resolved Majorana parity, (i) cannot be spontaneously broken at any non-vanishing temperature $T > 0$, (ii) is spontaneously broken at zero temperature $T = 0$. The free-energy argument underlying claim (i) is that there are gapped one-dimensional excitations of solitonic character in the many-body excitation spectrum of Hamiltonian (2.1) above the energy threshold M . Their Boltzmann weight at the temperature T is of order $e^{-M/T}$ so that their

average separation is of order

$$\xi(T) \sim e^{M/T}. \quad (5.1)$$

This length scale thus diverges exponentially fast upon approaching the zero-temperature limit at which long-range order associated to the spontaneous symmetry breaking of the symmetry (3.5) occurs.

Absence of spontaneous symmetry breaking of the symmetry (3.5) at any non-vanishing temperature T is a consequence of the local character of the symmetry (3.5) with respect to the label \mathfrak{m} . Spontaneous symmetry breaking of the symmetry (3.5) at $T = 0$ results from the global nature of the symmetry (3.5) with respect to imaginary time τ and the coordinate x .

The proof of claim (i) goes as follows. Integrating the Majorana fermions in the partition function (3.3) endows the dynamical field $\phi_{\mathfrak{m},\mathfrak{m}+1}(\tau, x)$ (that carries the engineering dimension of length⁻¹) with an effective action that must obey the symmetry (3.5).

The effective action for the dynamical field $\phi_{\mathfrak{m},\mathfrak{m}+1}(\tau, x)$ with a local Lagrangian density cannot contain a term such as

$$\mathcal{L}_\kappa := \kappa [\phi_{\mathfrak{m},\mathfrak{m}+1}(\tau, x) - \phi_{\mathfrak{m}+1,\mathfrak{m}+2}(\tau, x)]^2, \quad (5.2)$$

whereas a term like

$$\mathcal{L}_\zeta := \frac{\zeta}{M^2} [\phi_{\mathfrak{m},\mathfrak{m}+1}^2(\tau, x) - \phi_{\mathfrak{m}+1,\mathfrak{m}+2}^2(\tau, x)]^2 \quad (5.3)$$

is allowed by the symmetry (3.5). Here, the couplings κ and ζ are dimensionless. If we define the length scale

$$\ell := \frac{1}{M} \quad (5.4)$$

and assume that $\phi_{\mathfrak{m},\mathfrak{m}+1}$ has the two-soliton profile

$$\phi_{\mathfrak{m},\mathfrak{m}+1}(\tau, x) \propto \phi \left[\arctan\left(\frac{x+R}{\ell}\right) - \arctan\left(\frac{x-R}{\ell}\right) \right], \quad (5.5)$$

along the x direction ($\phi > 0$ is arbitrary), we find that, if $R \gg \ell$, the action penalties are given by

$$S_\kappa \sim \frac{\kappa \phi^2}{T} R \quad (5.6)$$

and

$$S_\zeta \sim \frac{\zeta \ell^2 \phi^4}{T} \ell, \quad (5.7)$$

respectively. At any non-vanishing temperature $T > 0$, the action penalty (5.6) causes the linear confinement of the pair of solitons, centered at R and $-R$, respectively. At any non-vanishing temperature $T > 0$, the action penalty (5.7) is independent of the separation R between the pair of solitons centered at R and $-R$, respectively,

i.e., solitons are deconfined. Thus, at any non-vanishing temperature $T > 0$, the thermal fluctuations that are encoded by the proliferation of solitons that interpolate between all the symmetry sectors of the symmetry (3.5) about any mean-field that breaks the symmetry (3.5) restore this symmetry.

The proof of claim (ii) goes as follows. At zero temperature, there is no contribution from the solitons owing to the finite energy of order of M needed to create them. The fact that the symmetry (3.5) is \mathfrak{m} -resolved is inoperative when $T = 0$. On the other hand, the symmetry (3.5) is global with respect to τ and x . Because it is Ising like, the effective quantum action at zero temperature can be thought of as a set of coupled Landau-Ginzburg actions, each one of which describes the classical Ising model in two-dimensional space and is labeled by the directed bond $\langle \mathfrak{m}, \mathfrak{m} + 1 \rangle$. Their coupling is controlled by the Majorana mass m_t for the triplet of Majorana fields (we are setting $m_s = 0$). Upon decoupling these classical Ising models in two-dimensional space by setting $m_t = 0$, we know from Sec. IV that the Ising symmetry is spontaneously broken. Switching on $m_t \neq 0$ only reinforces this spontaneous breaking of the Ising symmetry as the coupling induced by $m_t \neq 0$ is not frustrating.

It is instructive to establish the degeneracy of the ground state manifold that is spontaneously broken. In the limit

$$m_t = m_s = 0, \quad (5.8)$$

the Majorana modes decouple into the non-chiral pairs $\chi_{L,\mathfrak{m}}^\mu$ and $\chi_{R,\mathfrak{m}+1}^\mu$ with $\mu = 0, 1, 2, 3$, i.e., four flavors of Majorana fields of opposite chiralities for each directed bond $\langle \mathfrak{m}, \mathfrak{m} + 1 \rangle$. For each directed bond $\langle \mathfrak{m}, \mathfrak{m} + 1 \rangle$, the corresponding Majorana fields are strongly interacting through a $O(4)$ -symmetric Gross-Neveu interaction. However, the Majorana fields belonging to distinct directed bonds, say $\langle \mathfrak{m}, \mathfrak{m} + 1 \rangle$ and $\langle \mathfrak{m} + 1, \mathfrak{m} + 2 \rangle$, are decoupled. We may thus identify these pairs of interacting non-chiral Majorana modes as one-dimensional bundles labeled by the directed bond variable $\langle \mathfrak{m}, \mathfrak{m} + 1 \rangle$. Each bundle $\langle \mathfrak{m}, \mathfrak{m} + 1 \rangle$ can be bosonized. The interacting theory for the bundle $\langle \mathfrak{m}, \mathfrak{m} + 1 \rangle$ is characterized by the gap

$$\left\langle e^{i\sqrt{2\pi}(\hat{\varphi}_{L,\mathfrak{m}} + \hat{\varphi}_{R,\mathfrak{m}+1})} \right\rangle = \pm |M|^{1/2}. \quad (5.9)$$

The sign ambiguity on the right-hand side signals the breaking of a global \mathbb{Z}_2 symmetry for *each* bundle $\langle \mathfrak{m}, \mathfrak{m} + 1 \rangle$. Correspondingly, the soliton-like excitations are nothing but sine-Gordon solitons, i.e., domain walls separating regions along the x coordinate with different signs of the order parameter. From the point of view of the Majorana fermions $\chi_{L,\mathfrak{m}}^\mu$ and $\chi_{R,\mathfrak{m}+1}^\mu$ with $\mu = 0, 1, 2, 3$, different vacua are connected by the gauge transformation that changes a sign of either the left- or the right-moving Majorana fermion. As follows from Eqs. (4.10) and (4.11c), the Green's function $G_{LR}^{1d}(\tau, x)$ for a given bundle $\langle \mathfrak{m}, \mathfrak{m} + 1 \rangle$ is proportional to $\phi_{\mathfrak{m},\mathfrak{m}+1}$ on this bundle. At the mean-field level, $\phi_{\mathfrak{m},\mathfrak{m}+1}$ is nothing but an order

parameter that breaks the symmetry of the Hamiltonian under

$$\chi_{L,m}^\mu \chi_{R,m+1}^\mu \rightarrow \sigma_{L,m} \sigma_{R,m+1} \chi_{L,m}^\mu \chi_{R,m+1}^\mu, \quad \sigma_{L,m}, \sigma_{R,m+1} = \pm 1. \quad (5.10)$$

In other words, the sign of the Green's function (4.12c) is arbitrary. Choosing one sign breaks spontaneously a two-fold degeneracy for the bundle $\langle m, m+1 \rangle$. Given that there are n decoupled bundles of the form $\langle m, m+1 \rangle$, given the periodic boundary conditions identifying m with $m+n$, one deduces the degeneracy 2^n among all the possible symmetry breaking ground states that can be spontaneously selected.

However, the true degeneracy to be broken spontaneously in a system with periodic boundary conditions is 2^{n-1} once we switch on

$$m_t \neq 0 \quad (5.11)$$

while retaining $m_s = 0$. The symmetry (3.5) allows us to freely change the sign of the mean-field order parameter

$$\phi_{m',m'+1}(\tau, x) = \sigma_{m'} \sigma_{m'+1} \phi, \quad m' = 1, \dots, n, \quad \phi > 0, \quad (5.12)$$

for each bundle $\langle m, m+1 \rangle$, as long as the global condition

$$\prod_{m'=1}^n \phi_{m',m'+1}(\tau, x) = \pm \phi^n \quad (5.13)$$

is satisfied. The sign on the right-hand side of Eq. (5.13) is a gauge invariant quantity. The global condition reduces the number of choices by half, hence the 2^{n-1} ground state degeneracy when $m_t \neq 0$. [Notice that, when $m_s = m_t = 0$, symmetry (3.6) can be used instead of symmetry (3.5), in which case condition (5.13) does not apply anymore.]

The symmetry (3.5) thus implies that the sign of the Green's function (4.12c) remains arbitrary even if the bundles $\langle m, m+1 \rangle$ and $\langle m+1, m+2 \rangle$ are coupled by having $m_t \neq 0$. As we have explained above, it follows that the solitons, whose existence is guaranteed from bosonization when $m_t = 0$, are not confined by the interactions induced by a $m_t \neq 0$. On the other hand, the amplitude of the order parameter undergoes a change in magnitude in a region of size (5.4) around the soliton core. The soliton energy is sensitive to any change of amplitude in the order parameter. This is to say that solitons from different bundles $\langle m, m+1 \rangle$ and $\langle m+1, m+2 \rangle$ interact when $m_t \neq 0$. Because solitons cost energy which magnitude is bounded from below by the energy scale of the order of M , their average separation $\xi(T)$ is given by Eq. (5.1) at any non-vanishing temperature $T > 0$. The divergence of $\xi(T)$ in Eq. (5.1) is a signature of the onset of long-range order at $T = 0$ that breaks spontaneously the symmetry (3.5). Kitaev's honeycomb model also has an exponentially large correlation length at $T > 0$ related to the thermal creation of local defects, "visons" that are localized on the plaquette of the honeycomb lattice. In that model the defects are not mobile. In our case they are, although their mobility is one dimensional.

This proof can be generalized to any perturbation local in the spin operators, as those described in Secs. VI and VII. The proof holds since such perturbations are invariant with respect to a simultaneous change of sign of the left- and right-moving Majoranas on a given two-leg ladder m . Our model has two sectors: the spin sector and the fermionic one. In the latter sector, one is allowed to have operators which include odd numbers of Majorana fermions on a given two-leg ladder m . In the spin sector this is not allowed. In the microscopic derivation which starts with the lattice Hamiltonian of spins as in Secs. VI and VII, we arrive to the spin sector only. Hence, the 2^{n-1} -degeneracy described above is not directly observable in the spin sector of our model, that is in the subspace of the Hilbert space generated by the local spin operators.

VI. A SINGLE TWO-LEG LADDER

A. Microscopic lattice model and its continuum limit

Consider the following quantum spin-1/2 Hamiltonian on a (two-leg) ladder

$$\hat{H}_{\text{ladder}} := \hat{H}_{\text{leg}} + \hat{H}'_{\text{leg}} + \hat{H}_{\text{rung}} + \hat{H}_{\text{cross}} + \hat{H}_{\text{four-spin}}. \quad (6.1a)$$

The first leg of the ladder hosts the quantum spin-1/2 operators \hat{S}_i on every site $i = 1, \dots, N$, where any two consecutive sites is displaced by the lattice spacing a . Similarly, the second leg of the ladder hosts the quantum spin-1/2 operators $\hat{S}'_{i'}$ on every site $i' = 1, \dots, N$. Hamiltonians \hat{H}_{leg} and \hat{H}'_{leg} are a pair of decoupled quantum spin-1/2 antiferromagnetic Heisenberg model at criticality given by

$$\hat{H}_{\text{leg}} := \sum_{i=1}^N J_1 \hat{S}_i \cdot \hat{S}_{i+1} \quad (6.1b)$$

and

$$\hat{H}'_{\text{leg}} := \sum_{i=1}^N J_1 \hat{S}'_i \cdot \hat{S}'_{i+1} \quad (6.1c)$$

with $J_1 \geq 0$, respectively. The quantum spin-1/2 operators on the two legs also interact through a $SU(2)$ -symmetric Heisenberg exchange interaction for each rung

$$\hat{H}_{\text{rung}} := \sum_{i=1}^N J_{\perp} \hat{S}_i \cdot \hat{S}'_i \quad (6.1d)$$

with $\text{sgn}(J_{\perp})$ arbitrary, a cross-type interaction for each plaquette

$$\hat{H}_{\text{cross}} := \sum_{i=1}^N \left(J_{\setminus} \hat{S}_i \cdot \hat{S}'_{i+1} + J_{/} \hat{S}_{i+1} \cdot \hat{S}'_i \right) \quad (6.1e)$$

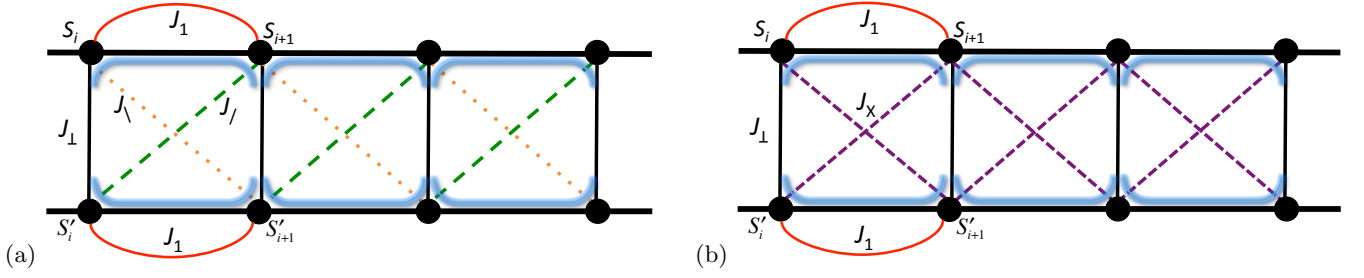


FIG. 8. (Color online) (a) Two quantum spin-1/2 chains can be arranged into a two-leg ladder. The intra-chain couplings J_1 are defined in Eqs. (6.1b) and (6.1c). The inter-chain couplings J_\perp (represented by the vertical black bond), J_\setminus (represented by the dashed orange bond), and $J_/$ (represented by the dashed green bond) are defined in Eqs. (6.1d) and (6.1e). The inter-chain four-spin coupling J_U (represented by the blue open-bracket) is defined in Eq. (6.1f). (b) The special case of Fig. 8(a) under the condition (6.9). Here, $J_x = -J_\perp/2$.

with $\text{sgn}(J_\setminus J_/)$ arbitrary, and a four-spin interaction for each plaquette

$$\hat{H}_{\text{four-spin}} := \sum_i^N J_U \left(\hat{\mathbf{S}}_i \cdot \hat{\mathbf{S}}_{i+1} \right) \left(\hat{\mathbf{S}}'_i \cdot \hat{\mathbf{S}}'_{i+1} \right) \quad (6.1f)$$

with $\text{sgn}(J_U)$ arbitrary. Hamiltonian (6.1) has the following symmetries.

There is the global unitary $SU(2)$ symmetry generated by the spin operator

$$\hat{\mathbf{S}}_{\text{tot}} := \hat{\mathbf{S}} + \hat{\mathbf{S}}', \quad (6.2a)$$

where

$$\hat{\mathbf{S}} := \sum_{i=1}^N \hat{\mathbf{S}}_i, \quad \hat{\mathbf{S}}' := \sum_{i=1}^N \hat{\mathbf{S}}'_i. \quad (6.2b)$$

We also note that the sum of Hamiltonians (6.1b) and (6.1c) has a global $SU(2) \times SU(2)$ symmetry generated independently by $\hat{\mathbf{S}}$ and $\hat{\mathbf{S}}'$, respectively. This global symmetry is broken down to the diagonal subgroup with the generator (6.2) by the interactions (6.1d), (6.1e), and (6.1f).

There is the global anti-unitary symmetry under time reversal under which

$$\hat{\mathbf{S}}_i \mapsto -\hat{\mathbf{S}}_i, \quad \hat{\mathbf{S}}'_i \mapsto -\hat{\mathbf{S}}'_i, \quad (6.3)$$

for all $i = 1, \dots, N$.

When the condition

$$J_\setminus = J_/ \equiv J_x \quad (6.4)$$

holds, there are two additional involutive (\mathbb{Z}_2) symmetries.

Under condition (6.4), Hamiltonian (6.1) is invariant under the transformation

$$\hat{\mathbf{S}}_i \mapsto \hat{\mathbf{S}}'_i, \quad \hat{\mathbf{S}}'_i \mapsto \hat{\mathbf{S}}_i, \quad (6.5)$$

for all $i = 1, \dots, N$.

Finally, if PBC are imposed together with the condition (6.4), Hamiltonian \hat{H}_{ladder} is invariant under all lattice translations generated by

$$\hat{\mathbf{S}}_i \mapsto \hat{\mathbf{S}}_{i+1}, \quad \hat{\mathbf{S}}'_i \mapsto \hat{\mathbf{S}}'_{i+1}, \quad (6.6)$$

for all $i = 1, \dots, N$.

Figure 8 depicts \hat{H}_{ladder} (6.1). This Hamiltonian was studied in Refs. 24 and 25. We also refer the reader to Chapter 21 of Ref. 26 and the Chapter 36 of Ref. 27 for some aspects of \hat{H}_{ladder} .

The naive continuum limit $\hat{\mathcal{H}}_{\text{ladder}}$ of \hat{H}_{ladder} defined by Eq. (6.1) is a $\widehat{su}(2)_1 \oplus \widehat{su}(2)_1$ Wess-Zumino-Novikov-Witten (WZNW) model perturbed by local interactions. For the upper leg, it is obtained by making the replacements

$$i \mathbf{a} \rightarrow x, \quad N \mathbf{a} \rightarrow L, \quad (6.7a)$$

where the sites of the upper leg of the ladder are $i = 1, \dots, N$ with N even and

$$\hat{\mathbf{S}}_{2i} \rightarrow \mathbf{a} \left[\hat{\mathbf{J}}_L(x) + \hat{\mathbf{J}}_R(x) + \hat{\mathbf{n}}(x) \right], \quad (6.7b)$$

$$\hat{\mathbf{S}}_{2i+1} \rightarrow \mathbf{a} \left[\hat{\mathbf{J}}_L(x) + \hat{\mathbf{J}}_R(x) - \hat{\mathbf{n}}(x) \right], \quad (6.7c)$$

$$(-1)^i \hat{\mathbf{S}}_i \cdot \hat{\mathbf{S}}_{i+1} \rightarrow \mathbf{a} \hat{\varepsilon}(x), \quad (6.7d)$$

for all sites $i = 1, \dots, N/2$ of the upper leg, assuming that N is even. The left- and right- moving currents $\hat{\mathbf{J}}_L$ and $\hat{\mathbf{J}}_R$ generate the $\widehat{su}(2)_1$ affine Lie algebra of the $c = 1$ quantum critical point of the nearest-neighbor anti-ferromagnetic quantum spin-1/2 chain. The fields $\hat{\mathbf{n}}$ and $\hat{\varepsilon}$ have anomalous scaling exponents 1/2 at this quantum critical point. The same replacements are done after adding a prime to the sites and the quantum spin-1/2 hosted by the lower leg of the ladder. Hereto, the left- and right- moving currents $\hat{\mathbf{J}}'_L$ and $\hat{\mathbf{J}}'_R$ generate another $\widehat{su}(2)_1$ affine Lie algebra, while the fields $\hat{\mathbf{n}}'$ and $\hat{\varepsilon}'$ have the anomalous scaling dimensions 1/2 at this quantum critical point. The perturbation to the $\widehat{su}(2)_1 \oplus \widehat{su}(2)_1$

WZNW model with the conserved currents $\widehat{\mathbf{J}}_L, \widehat{\mathbf{J}}_R, \widehat{\mathbf{J}}'_L$, and $\widehat{\mathbf{J}}'_R$ is

$$\begin{aligned} \widehat{\mathcal{V}}(x) := & g_{nn} \widehat{\mathbf{n}}(x) \cdot \widehat{\mathbf{n}}'(x) + g_{\varepsilon\varepsilon} \widehat{\varepsilon}(x) \widehat{\varepsilon}'(x) \\ & + g_{jj} \left(\widehat{\mathbf{J}}_L(x) \cdot \widehat{\mathbf{J}}'_L(x) + \widehat{\mathbf{J}}_R(x) \cdot \widehat{\mathbf{J}}'_R(x) \right) \\ & + g_{jj} \left(\widehat{\mathbf{J}}_L(x) \cdot \widehat{\mathbf{J}}'_R(x) + \widehat{\mathbf{J}}_R(x) \cdot \widehat{\mathbf{J}}'_L(x) \right) \\ & + g_{\text{tw},n} \widehat{\mathbf{n}}(x) \cdot \partial_x \widehat{\mathbf{n}}'(x) + g_{\text{tw},\varepsilon} \widehat{\varepsilon}(x) \partial_x \widehat{\varepsilon}'(x) \end{aligned} \quad (6.8a)$$

up to irrelevant local perturbations. Here, the bare values of the couplings are

$$g_{nn} \equiv \left(g_{nn}^\perp + g'_{nn} + g_{nn}^\setminus \right) \quad (6.8b)$$

$$= 2 \times \mathbf{a} \left(J_\perp - J_J - J_\setminus \right) \quad (6.8c)$$

for the inter-chain staggered magnetization coupling,

$$g_{\varepsilon\varepsilon} \equiv \mathbf{a} J_U \quad (6.8d)$$

for the inter-chain dimerization coupling,

$$\begin{aligned} g_{jj} & \equiv \left(g_{jj}^\perp + g'_{jj} + g_{jj}^\setminus \right) \\ & = 2 \times \mathbf{a} \left(J_\perp + J_J + J_\setminus \right) \end{aligned} \quad (6.8e)$$

for the inter-chain conformal current coupling,

$$\begin{aligned} g_{\text{tw},n} & \equiv \left(g'_{\text{tw},n} - g_{\text{tw},n}^\setminus \right) \\ & = \mathbf{a}^2 \left(J_J - J_\setminus \right) \end{aligned} \quad (6.8f)$$

for the inter-chain twisted magnetization coupling, and

$$g_{\text{tw},\varepsilon} \equiv 0 \quad (6.8g)$$

for the inter-chain twisted dimerization coupling.

The bare value of the inter-chain conformal current coupling vanishes if ²⁴

$$J_\perp = - \left(J_J + J_\setminus \right). \quad (6.9a)$$

The bare value of the inter-chain twist magnetization coupling vanishes if ²⁸

$$J_J = J_\setminus \equiv J_\times. \quad (6.9b)$$

If we impose conditions (6.9), then the effective local interaction (6.8) simplifies to

$$\widehat{\mathcal{V}}_{\text{tuned}}(x) := g_{nn}^{\text{tuned}} \widehat{\mathbf{n}}(x) \cdot \widehat{\mathbf{n}}'(x) + g_{\varepsilon\varepsilon} \widehat{\varepsilon}(x) \widehat{\varepsilon}'(x), \quad (6.10a)$$

where

$$g_{nn}^{\text{tuned}} := 4 \times \mathbf{a} J_\perp, \quad g_{\varepsilon\varepsilon} := \mathbf{a} J_U. \quad (6.10b)$$

We depict the model $\widehat{H}_{\text{ladder}}$ (6.1) under the condition (6.9) in Fig. 8(b). Its symmetry under transformations (6.5) or (6.6) carries over in the continuum limit to the symmetry by which unprimed and primed fields are exchanged or under sign reversal of the staggered fields, respectively.

B. Abelian bosonization

To proceed, we follow Ref. 24 and apply the Abelian bosonization rules on the tuned interaction density (6.10). To this end, we consider the upper leg (lower leg) of the ladder and introduce the pair of bosonic quantum fields $\widehat{\phi}(t, x)$ and $\widehat{\theta}(t, x)$ ($\widehat{\phi}'(t, x)$ and $\widehat{\theta}'(t, x)$) by demanding that they obey the equal-time algebra

$$\left[\widehat{\phi}(t, x), \widehat{\theta}(t, x') \right] = -\frac{i}{2} \text{sgn}(x - x'), \quad \left[\widehat{\phi}'(t, x), \widehat{\theta}'(t, x') \right] = -\frac{i}{2} \text{sgn}(x - x'), \quad (6.11a)$$

for any $t \in \mathbb{R}$, and $0 \leq x, x' \leq L_x$. The equal-time commutators between unprimed and primed fields are all vanishing. The two pairs of bosonic fields are related to the staggered magnetization and staggered dimerization by

$$\widehat{n}^x = +\frac{1}{\pi\mathbf{a}} \cos \left(\sqrt{2\pi} \widehat{\theta} \right), \quad \widehat{n}^y = +\frac{1}{\pi\mathbf{a}} \sin \left(\sqrt{2\pi} \widehat{\theta} \right), \quad \widehat{n}^z = -\frac{1}{\pi\mathbf{a}} \sin \left(\sqrt{2\pi} \widehat{\phi} \right), \quad \widehat{\varepsilon} = +\frac{1}{\pi\mathbf{a}} \cos \left(\sqrt{2\pi} \widehat{\phi} \right), \quad (6.11b)$$

for the upper leg of the ladder and by

$$\widehat{n}'^x = +\frac{1}{\pi\mathbf{a}} \cos \left(\sqrt{2\pi} \widehat{\theta}' \right), \quad \widehat{n}'^y = +\frac{1}{\pi\mathbf{a}} \sin \left(\sqrt{2\pi} \widehat{\theta}' \right), \quad \widehat{n}'^z = -\frac{1}{\pi\mathbf{a}} \sin \left(\sqrt{2\pi} \widehat{\phi}' \right), \quad \widehat{\varepsilon}' = +\frac{1}{\pi\mathbf{a}} \cos \left(\sqrt{2\pi} \widehat{\phi}' \right), \quad (6.11c)$$

for the lower leg of the ladder. After some algebra, we arrive at the Abelian bosonized representation of the $\widehat{su}(2)_1 \oplus \widehat{su}(2)_1$ WZNW model with the conserved currents $\widehat{\mathbf{J}}_L, \widehat{\mathbf{J}}_R, \widehat{\mathbf{J}}'_L$, and $\widehat{\mathbf{J}}'_R$ perturbed by the intra-ladder tuned interaction

density (6.10) that is given by the Hamiltonian density

$$\widehat{\mathcal{H}} := \widehat{\mathcal{H}}_{\text{leg}}^{\text{upper}} + \widehat{\mathcal{H}}_{\text{leg}}^{\text{lower}} + \widehat{\mathcal{H}}_{\text{intra-ladder}}, \quad (6.12a)$$

$$\widehat{\mathcal{H}}_{\text{leg}}^{\text{upper}} := \frac{v}{2} \left[\widehat{\Pi}^2 + \left(\partial_x \widehat{\phi} \right)^2 \right], \quad \widehat{\mathcal{H}}_{\text{leg}}^{\text{lower}} := \frac{v}{2} \left[\widehat{\Pi}'^2 + \left(\partial_x \widehat{\phi}' \right)^2 \right], \quad (6.12b)$$

$$\widehat{\mathcal{H}}_{\text{intra-ladder}} := -\frac{g_{nn}^{\text{tuned}} - g_{\varepsilon\varepsilon}}{2(\pi\mathbf{a})^2} \cos \left(\sqrt{2\pi} \left(\widehat{\phi} + \widehat{\phi}' \right) \right) + \frac{g_{nn}^{\text{tuned}} + g_{\varepsilon\varepsilon}}{2(\pi\mathbf{a})^2} \cos \left(\sqrt{2\pi} \left(\widehat{\phi} - \widehat{\phi}' \right) \right) + \frac{g_{nn}^{\text{tuned}}}{(\pi\mathbf{a})^2} \cos \left(\sqrt{2\pi} \left(\widehat{\theta} - \widehat{\theta}' \right) \right). \quad (6.12c)$$

Here, we must supplement the equal-time algebra (6.11a) by the canonical bosonic equal-time commutators

$$\left[\widehat{\phi}(t, x), \widehat{\Pi}(t, x') \right] = i\delta(x - x'), \quad \left[\widehat{\phi}'(t, x), \widehat{\Pi}'(t, x') \right] = i\delta(x - x'), \quad (6.12d)$$

with

$$\widehat{\Pi}(t, x') := \left(v^{-1} \partial_t \widehat{\phi} \right) (t, x'), \quad \widehat{\Pi}'(t, x') := \left(v^{-1} \partial_t \widehat{\phi}' \right) (t, x'). \quad (6.12e)$$

The symmetry under the transformation (6.5) follows from the invariance of the bosonic theory defined by Eq. (6.12) under the transformation

$$\widehat{\theta} \mapsto \widehat{\theta}', \quad \widehat{\phi} \mapsto \widehat{\phi}', \quad \widehat{\theta}' \mapsto \widehat{\theta}, \quad \widehat{\phi}' \mapsto \widehat{\phi}. \quad (6.13)$$

The symmetry under the transformation (6.6) follows from the invariance of the bosonic theory defined by Eq. (6.12) under the transformation

$$\widehat{\phi} \mapsto \widehat{\phi} + \sqrt{\frac{\pi}{2}}, \quad \widehat{\theta} \mapsto \widehat{\theta} + \sqrt{\frac{\pi}{2}}, \quad \widehat{\phi}' \mapsto \widehat{\phi}' + \sqrt{\frac{\pi}{2}}, \quad \widehat{\theta}' \mapsto \widehat{\theta}' + \sqrt{\frac{\pi}{2}}. \quad (6.14)$$

C. Majorana representation

Left- and right-moving Majorana fields are defined by

$$\widehat{\chi}_{\text{L}}^1 := \frac{1}{\sqrt{\pi\mathbf{a}}} \cos \left(\sqrt{4\pi} \widehat{\phi}_{+, \text{L}} \right) \equiv \frac{1}{\sqrt{\pi\mathbf{a}}} \cos \left(\sqrt{\pi} \left(\widehat{\phi}_+ + \widehat{\theta}_+ \right) \right) \equiv \frac{1}{\sqrt{\pi\mathbf{a}}} \cos \left(\sqrt{\frac{\pi}{2}} \left(\widehat{\phi} + \widehat{\phi}' + \widehat{\theta} + \widehat{\theta}' \right) \right), \quad (6.15a)$$

$$\widehat{\chi}_{\text{L}}^2 := \frac{-1}{\sqrt{\pi\mathbf{a}}} \sin \left(\sqrt{4\pi} \widehat{\phi}_{+, \text{L}} \right) \equiv \frac{-1}{\sqrt{\pi\mathbf{a}}} \sin \left(\sqrt{\pi} \left(\widehat{\phi}_+ + \widehat{\theta}_+ \right) \right) \equiv \frac{-1}{\sqrt{\pi\mathbf{a}}} \sin \left(\sqrt{\frac{\pi}{2}} \left(\widehat{\phi} + \widehat{\phi}' + \widehat{\theta} + \widehat{\theta}' \right) \right), \quad (6.15b)$$

$$\widehat{\chi}_{\text{L}}^3 := \frac{1}{\sqrt{\pi\mathbf{a}}} \cos \left(\sqrt{4\pi} \widehat{\phi}_{-, \text{L}} \right) \equiv \frac{1}{\sqrt{\pi\mathbf{a}}} \cos \left(\sqrt{\pi} \left(\widehat{\phi}_- + \widehat{\theta}_- \right) \right) \equiv \frac{1}{\sqrt{\pi\mathbf{a}}} \cos \left(\sqrt{\frac{\pi}{2}} \left(\widehat{\phi} - \widehat{\phi}' + \widehat{\theta} - \widehat{\theta}' \right) \right), \quad (6.15c)$$

$$\widehat{\chi}_{\text{L}}^0 := \frac{-1}{\sqrt{\pi\mathbf{a}}} \sin \left(\sqrt{4\pi} \widehat{\phi}_{-, \text{L}} \right) \equiv \frac{-1}{\sqrt{\pi\mathbf{a}}} \sin \left(\sqrt{\pi} \left(\widehat{\phi}_- + \widehat{\theta}_- \right) \right) \equiv \frac{-1}{\sqrt{\pi\mathbf{a}}} \sin \left(\sqrt{\frac{\pi}{2}} \left(\widehat{\phi} - \widehat{\phi}' + \widehat{\theta} - \widehat{\theta}' \right) \right), \quad (6.15d)$$

and

$$\widehat{\chi}_{\text{R}}^1 := \frac{1}{\sqrt{\pi\mathbf{a}}} \cos \left(\sqrt{4\pi} \widehat{\phi}_{+, \text{R}} \right) \equiv \frac{1}{\sqrt{\pi\mathbf{a}}} \cos \left(\sqrt{\pi} \left(\widehat{\phi}_+ - \widehat{\theta}_+ \right) \right) \equiv \frac{1}{\sqrt{\pi\mathbf{a}}} \cos \left(\sqrt{\frac{\pi}{2}} \left(\widehat{\phi} + \widehat{\phi}' - \widehat{\theta} - \widehat{\theta}' \right) \right), \quad (6.15e)$$

$$\widehat{\chi}_{\text{R}}^2 := \frac{1}{\sqrt{\pi\mathbf{a}}} \sin \left(\sqrt{4\pi} \widehat{\phi}_{+, \text{R}} \right) \equiv \frac{1}{\sqrt{\pi\mathbf{a}}} \sin \left(\sqrt{\pi} \left(\widehat{\phi}_+ - \widehat{\theta}_+ \right) \right) \equiv \frac{1}{\sqrt{\pi\mathbf{a}}} \sin \left(\sqrt{\frac{\pi}{2}} \left(\widehat{\phi} + \widehat{\phi}' - \widehat{\theta} - \widehat{\theta}' \right) \right), \quad (6.15f)$$

$$\widehat{\chi}_{\text{R}}^3 := \frac{1}{\sqrt{\pi\mathbf{a}}} \cos \left(\sqrt{4\pi} \widehat{\phi}_{-, \text{R}} \right) \equiv \frac{1}{\sqrt{\pi\mathbf{a}}} \cos \left(\sqrt{\pi} \left(\widehat{\phi}_- - \widehat{\theta}_- \right) \right) \equiv \frac{1}{\sqrt{\pi\mathbf{a}}} \cos \left(\sqrt{\frac{\pi}{2}} \left(\widehat{\phi} - \widehat{\phi}' - \widehat{\theta} + \widehat{\theta}' \right) \right), \quad (6.15g)$$

$$\widehat{\chi}_{\text{R}}^0 := \frac{1}{\sqrt{\pi\mathbf{a}}} \sin \left(\sqrt{4\pi} \widehat{\phi}_{-, \text{R}} \right) \equiv \frac{1}{\sqrt{\pi\mathbf{a}}} \sin \left(\sqrt{\pi} \left(\widehat{\phi}_- - \widehat{\theta}_- \right) \right) \equiv \frac{1}{\sqrt{\pi\mathbf{a}}} \sin \left(\sqrt{\frac{\pi}{2}} \left(\widehat{\phi} - \widehat{\phi}' - \widehat{\theta} + \widehat{\theta}' \right) \right), \quad (6.15h)$$

respectively.

After some algebra, we arrive at the Majorana representation of the $\widehat{su}(2)_1 \oplus \widehat{su}(2)_1$ WZNW model with the

conserved currents $\hat{\mathbf{J}}_L$, $\hat{\mathbf{J}}_R$, $\hat{\mathbf{J}}'_L$, and $\hat{\mathbf{J}}'_R$ perturbed by the intra-ladder interaction density (6.10) that is given by

$$\hat{\mathcal{H}}_{\text{ladder}}^{\text{tuned}} := \sum_{\mu=0,1,2,3} \hat{\mathcal{H}}_{\text{ladder},\mu}^{\text{tuned}} \quad (6.16a)$$

with

$$\hat{\mathcal{H}}_{\text{ladder},\mu}^{\text{tuned}} := \frac{i}{2} v (\hat{\chi}_L^\mu \partial_x \hat{\chi}_L^\mu - \hat{\chi}_R^\mu \partial_x \hat{\chi}_R^\mu) + i m_\mu^{\text{tuned}} \hat{\chi}_L^\mu \hat{\chi}_R^\mu, \quad (6.16b)$$

where

$$v \propto J_1 \mathbf{a} \quad (6.16c)$$

and

$$m_\mu^{\text{tuned}} = \begin{cases} m_s^{\text{tuned}}, & \mu = 0, \\ m_t^{\text{tuned}}, & \mu = 1, 2, 3. \end{cases} \quad (6.16d)$$

The singlet mass m_s^{tuned} and the triplet mass m_t^{tuned} are here given by

$$\begin{aligned} m_s^{\text{tuned}} &:= \frac{-1}{2\pi\mathbf{a}} (3g_{nn}^{\text{tuned}} + g_{\varepsilon\varepsilon}) \\ &= \frac{-1}{2\pi} (12J_\perp + J_U), \end{aligned} \quad (6.17a)$$

$$\begin{aligned} m_t^{\text{tuned}} &:= \frac{1}{2\pi\mathbf{a}} (g_{nn}^{\text{tuned}} - g_{\varepsilon\varepsilon}) \\ &= \frac{1}{2\pi} (4J_\perp - J_U), \end{aligned} \quad (6.17b)$$

respectively. Upon tuning the ratio of J_U/J_\perp such that the singlet (triplet) mass m_s^{tuned} (m_t^{tuned}) vanish, we achieve the critical point with central charge 1/2 (3/2) in a single ladder (6.1).

The symmetry under the transformation (6.5) is represented by the invariance of the Majorana theory defined by Eq. (6.16) under the transformation

$$\hat{\chi}_M^1 \mapsto \hat{\chi}_M^1, \quad (6.18a)$$

$$\hat{\chi}_M^2 \mapsto \hat{\chi}_M^2, \quad (6.18b)$$

$$\hat{\chi}_M^3 \mapsto \hat{\chi}_M^3, \quad (6.18c)$$

$$\hat{\chi}_M^0 \mapsto -\hat{\chi}_M^0, \quad (6.18d)$$

for any $M = L, R$.

The symmetry under the transformation (6.6) is represented in a trivial way for the Majorana theory defined by Eq. (6.16), for the transformation (6.6) is represented by the identity

$$\hat{\chi}_M^\mu \mapsto \hat{\chi}_M^\mu \quad (6.19)$$

for any $\mu = 0, 1, 2, 3$ and $M = L, R$ according to Eq. (6.15).

We follow Ref. 25 to discuss the nature of the phase transition. According to the sign of the singlet mass and the triplet mass at the fine-tuned point (6.17), we sketch the phase diagram in Fig. 9(a). There are 9 pairs of the

signature of m_s and m_t . These 9 pairs label 4 phases, 4 critical line and 1 trivial point at the origin. In Fig. 9(b) a refined version of the phase diagram in Fig. 9(a) is obtained by considering the difference of the magnitude of the singlet mass and the triplet mass. As long as $|m_s| > |m_t|$, namely the triplet branch of the spectrum remain the lowest, the phase is related to the phase of the bilinear and biquadratic spin-1 chain. We note that the dashed green line is the mirror image of the blue line around the J_U axis. We also remark that the dashed green line is not present in Fig. 9(a).

VII. COUPLED TWO-LEG LADDERS

A. Microscopic lattice model and its continuum limit

We consider the following inter-ladder interaction

$$\hat{H}_{\text{inter-ladder}} := \hat{H}_\Delta + \hat{H}'_\Delta + \hat{H}_\square + \hat{H}'_\square, \quad (7.1a)$$

where

$$\begin{aligned} \hat{H}_\Delta &:= \frac{J_\chi}{2} \sum_{i=1}^N \sum_{m=1}^{n-1} \left[\hat{\mathbf{S}}_{i,m+1} \cdot \left(\hat{\mathbf{S}}_{i+1,m} \wedge \hat{\mathbf{S}}_{i,m} \right) \right. \\ &\quad \left. + \hat{\mathbf{S}}_{i+1,m} \cdot \left(\hat{\mathbf{S}}_{i,m+1} \wedge \hat{\mathbf{S}}_{i+1,m+1} \right) \right] \end{aligned} \quad (7.1b)$$

and

$$\begin{aligned} \hat{H}_\square &:= J_\vee \sum_{i=1}^N \sum_{m=1}^{n-1} \left(\hat{\mathbf{S}}_{i,m} \cdot \hat{\mathbf{S}}_{i,m+1} \right. \\ &\quad \left. + \kappa_\vee \hat{\mathbf{S}}_{i,m+1} \cdot \hat{\mathbf{S}}_{i+1,m} + \kappa_\wedge \hat{\mathbf{S}}_{i,m} \cdot \hat{\mathbf{S}}_{i+1,m+1} \right), \end{aligned} \quad (7.1c)$$

with \hat{H}'_Δ and \hat{H}'_\square deduced from \hat{H}_Δ and \hat{H}_\square by the substitution $\hat{\mathbf{S}}_{i,m} \rightarrow \hat{\mathbf{S}}'_{i,m}$. The couplings κ_\vee and κ_\wedge are dimensionless. (The choice $\kappa_\vee = \kappa_\wedge = 1/2$ is shown in Fig. 2.)

The inter-ladder Hamiltonian (7.1) has a global $SU(2) \times SU(2)$ symmetry that reflects the fact that there is no coupling between the quantum spin $\hat{\mathbf{S}}_{i,m}$ and the quantum spin $\hat{\mathbf{S}}'_{i',m+1}$ for all $i, i' = 1, \dots, N$.

For the same reason, the inter-ladder Hamiltonian (7.1) has a global \mathbb{Z}_2 symmetry under the transformation [recall Eq. (6.5)]

$$\hat{\mathbf{S}}_{i,m} \mapsto \hat{\mathbf{S}}'_{i,m}, \quad \hat{\mathbf{S}}'_{i,m} \mapsto \hat{\mathbf{S}}_{i,m}, \quad (7.2)$$

for $i = 1, \dots, N$ and $m = 1, \dots, n$.

If PBC are imposed on the indices i , the inter-ladder Hamiltonian (7.1) is then invariant under all lattice translations generated by the transformation [recall Eq. (6.6)]

$$\hat{\mathbf{S}}_{i,m} \mapsto \hat{\mathbf{S}}_{i+1,m}, \quad \hat{\mathbf{S}}'_{i,m} \mapsto \hat{\mathbf{S}}'_{i+1,m}, \quad (7.3)$$

$i = 1, \dots, N$ and $m = 1, \dots, n$.

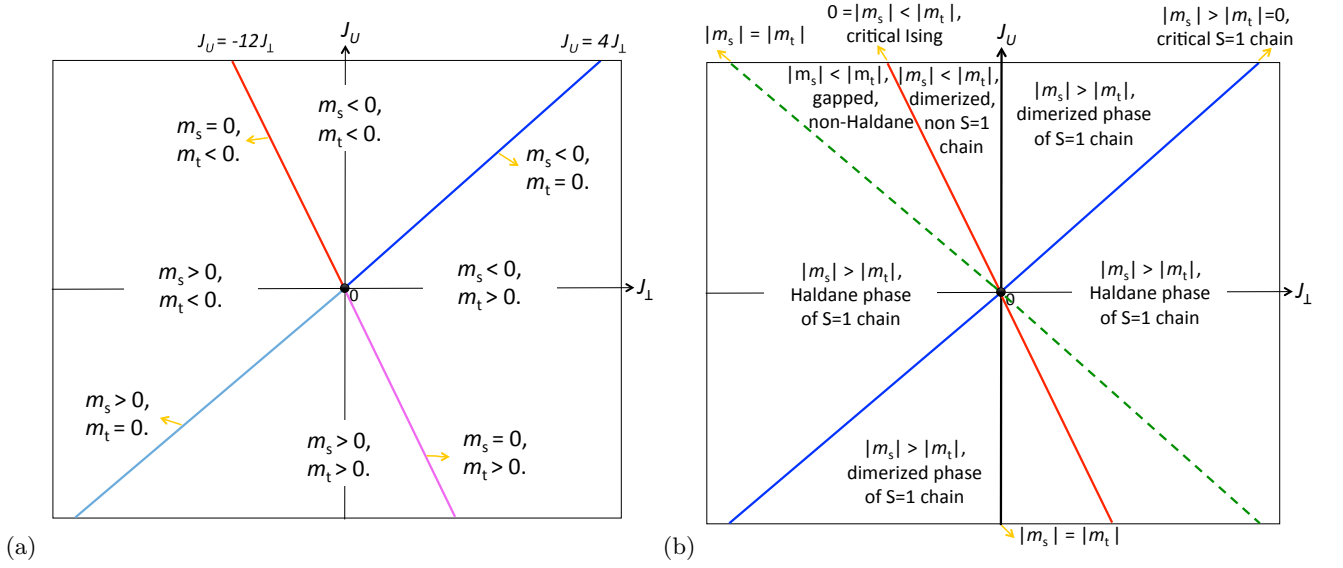


FIG. 9. (Color online) (a) Phase diagram of the fine-tuned quantum spin-1/2 ladder (6.9) based on the sign of the singlet mass and the triplet mass (6.17). (b) A refined version of the phase diagram in Fig. 9(a) is obtained by considering the difference of the magnitude of the singlet mass and the triplet mass. As long as $|m_s| > |m_t|$, namely the triplet branch of the spectrum remains the lowest, the phase is related to the phase of the bilinear and biquadratic spin-1 chain.

Finally, the inter-ladder Hamiltonian (7.1) is invariant under reversal of time, a global anti-unitary transformation under which

$$\widehat{S}_{i,m} \rightarrow -\widehat{S}_{i,m}, \quad \widehat{S}'_{i',m'} \rightarrow -\widehat{S}'_{i',m'}, \quad (7.4a)$$

for all $i, i' = 1, \dots, N$ and $m, m' = 1, \dots, n$, combined with the transformation

$$J_\chi \mapsto -J_\chi. \quad (7.4b)$$

Any fixed non-vanishing J_χ breaks time-reversal symmetry.

The naive continuum limit of $\widehat{H}_{\text{inter-ladder}}$ defined by Eq. (7.1) was derived in Ref. 19 (see also Ref. 29). All the bare values of the coupling constants entering Eq. (7.1) that are relevant from the point of view of a one-loop renormalization group analysis at the WZNW critical point vanish at the fine-tuned point

$$\kappa_\lambda = \kappa_j = 1/2, \quad (7.5)$$

and the leading-order contribution is simply the current-current interaction

$$\widehat{\mathcal{H}}_{\Delta, \square}(x) := \sum_{m=1}^{n-1} \sum_{a=1}^3 \left\{ \lambda \left[\widehat{J}_{L,m}^a(x) \widehat{J}_{R,m+1}^a(x) + \widehat{J}_{L,m}^a(x) \widehat{J}_{R,m+1}^a(x) \right] + \tilde{\lambda} \left[\widehat{J}_{R,m}^a(x) \widehat{J}_{L,m+1}^a(x) + \widehat{J}_{R,m}^a(x) \widehat{J}_{L,m+1}^a(x) \right] \right\} \quad (7.6a)$$

with

$$\lambda = 2\mathbf{a} [(J_\chi/\pi) + 2J_V], \quad \tilde{\lambda} = 2\mathbf{a} [-(J_\chi/\pi) + 2J_V]. \quad (7.6b)$$

Here, $\widehat{J}_{M,m}^a(x) \in \widehat{su}(2)_{k=1}$ and $\widehat{J}'_{M,m}(x) \in \widehat{su}(2)_{k'=1}$ with $M = L, R$, i.e., their equal-time commutators are those of the affine Lie algebras $\widehat{su}(2)_{k=1}$ and $\widehat{su}(2)_{k'=1}$, respectively.

The global $SU(2) \times SU(2)$ symmetry of the inter-ladder Hamiltonian (7.1) is manifest in that there is no coupling between the currents $\widehat{J}_{M,m}^a(x)$ and $\widehat{J}'_{M,m+1}(x)$. They are related to the original quantum spin 1/2 by adding the

label m on both sides of Eqs. (6.7b), (6.7c), and (6.7d) for the unprimed fields, say.

The global \mathbb{Z}_2 symmetry under

$$\widehat{J}_{M,m}^a(x) \mapsto \widehat{J}'_{M,m}(x), \quad \widehat{J}'_{M,m}(x) \mapsto \widehat{J}_{M,m}^a(x) \quad (7.7)$$

is also manifest.

If PBC are imposed with respect to x , the symmetry of the inter-ladder Hamiltonian (7.1) under all lat-

tice translations generated by the transformation (7.3) is then also manifest in the continuum Hamiltonian density (7.6), since the currents $\hat{J}_{M,m}^a(x)$ and $\hat{J}_{M,m}^a(x)$ are unchanged by the transformation (7.3), unlike the staggered fields on the right-hand sides of Eqs. (6.7b), (6.7c), and (6.7d) for the unprimed fields, say.

Remarkably, the continuum Hamiltonian density (7.6) has acquired an emergent symmetry, namely it is invariant under the m -resolved transformations

$$\hat{n}_m \mapsto \sigma_m \hat{n}_m, \quad \hat{n}'_m \mapsto \sigma_m \hat{n}'_m, \quad (7.8a)$$

$$\hat{\varepsilon}_m \mapsto \sigma_m \hat{\varepsilon}_m, \quad \hat{\varepsilon}'_m \mapsto \sigma_m \hat{\varepsilon}'_m, \quad (7.8b)$$

where $\sigma_m = \pm 1$ for $m = 1, \dots, n$, unlike the microscopic inter-ladder Hamiltonian (7.1) for which the lattice translation (7.3) must act simultaneously on all ladder for it to leave the microscopic inter-ladder Hamiltonian (7.1) invariant.

Reversal of time is explicitly broken by any non-vanishing $\lambda \neq \tilde{\lambda}$.

Observe that the bare value of $\tilde{\lambda}$ vanishes if

$$\frac{J_\chi}{\pi} = 2J_V. \quad (7.9)$$

Upon the fine tuning (7.9), the current-current interaction (7.6a) simplifies to

$$\begin{aligned} \hat{H}_{\text{inter-ladder}}(x) := & \sum_{m=1}^{n-1} \sum_{a=1}^3 \lambda \left[\hat{J}_{L,m}^a(x) \hat{J}_{R,m+1}^a(x) \right. \\ & \left. + \hat{J}_{L,m}^a(x) \hat{J}_{R,m+1}^a(x) \right]. \end{aligned} \quad (7.10)$$

The interaction $\hat{H}_{\text{inter-ladder}}(x)$ is represented by the directed arcs in Fig. 4(a). The arrow on the arcs indicates that this choice of current-current interaction completely breaks time-reversal symmetry.

To summarize, we are considering a set of n ladders labeled by the index $m = 1, \dots, n$. We are assigning the coordinate $x \in \mathbb{R}$ along the direction of the leg to each ladder. The ladders are all parallel and equally spaced along a direction y perpendicular to the x axis. The Hamiltonian for this set of ladders is approximated by

$$\begin{aligned} \hat{H} := & \int_0^{L_x} dx \left[\sum_{m=1}^n \hat{H}_{\text{WZNW},m}(x) + \sum_{m=1}^n \hat{H}_{\text{intra-ladder},m}(x) \right. \\ & \left. + \sum_{m=1}^{n-1} \hat{H}_{\text{inter-ladder},m}(x) \right]. \end{aligned} \quad (7.11a)$$

The Hamiltonian density $\hat{H}_{\text{WZNW},m}(x)$ encodes the conformal-field theory in two-dimensional space time with the affine Lie algebra $\widehat{su}(2)_1 \oplus \widehat{su}(2)_1$. It describes a ladder at a quantum critical point with central charge

$c_m = 2$ where $m = 1, \dots, n$. The intra-ladder interaction is [c.f. Eq. (6.10)]

$$\begin{aligned} \hat{H}_{\text{intra-ladder},m}(x) := & g_{nn}^{\text{tuned}} \hat{n}_m(x) \cdot \hat{n}'_m(x) \\ & + g_{\varepsilon\varepsilon} \hat{\varepsilon}_m(x) \hat{\varepsilon}'_m(x). \end{aligned} \quad (7.11b)$$

The couplings g_{nn}^{tuned} and $g_{\varepsilon\varepsilon}$ are dimensionless. They are related to the microscopic data of the spin-1/2 ladder depicted in Fig. 2 by Eq. (6.10b). The inter-ladder interaction is [c.f. Eq. (7.10)]

$$\begin{aligned} \hat{H}_{\text{inter-ladder},m}(x) := & \sum_{a=1}^3 \lambda \left[\hat{J}_{L,m}^a(x) \hat{J}_{R,m+1}^a(x) \right. \\ & \left. + \hat{J}_{L,m}^a(x) \hat{J}_{R,m+1}^a(x) \right], \end{aligned} \quad (7.11c)$$

where $\hat{J}_{M,m}^a(x) \in \widehat{su}(2)_{k=1}$ and $\hat{J}_{M,m}^a(x) \in \widehat{su}(2)_{k'=1}$ with $M = L, R$, i.e., their equal-time commutators are those of the affine Lie algebras $\widehat{su}(2)_{k=1}$ and $\widehat{su}(2)_{k'=1}$, respectively. The coupling λ is dimensionless. It is related to the microscopic data of the spin-1/2 ladder depicted in Fig. 2 by Eq. (7.6b). The symmetries of Hamiltonian (7.11) are the following.

The local symmetry with the affine Lie algebra $\widehat{su}(2)_1 \oplus \widehat{su}(2)_1$ associated to $\hat{H}_{\text{WZNW}}(x)$ is reduced to the global $SU(2) \times SU(2)$ symmetry by the inter-ladder interaction densities, owing to its invariance under the interchange of unprimed and primed fields.

There is a global \mathbb{Z}_2 symmetry under the interchange of unprimed and primed fields.

If PBC are imposed, there is an emergent m -resolved \mathbb{Z}_2 symmetry under the transformation

$$\hat{n}_m \mapsto \sigma_m \hat{n}_m, \quad \hat{n}'_m \mapsto \sigma_m \hat{n}'_m, \quad (7.12a)$$

$$\hat{\varepsilon}_m \mapsto \sigma_m \hat{\varepsilon}_m, \quad \hat{\varepsilon}'_m \mapsto \sigma_m \hat{\varepsilon}'_m, \quad (7.12b)$$

$$\hat{J}_{M,m} \mapsto \hat{J}_{M,m}, \quad \hat{J}_{M,m} \mapsto \hat{J}_{M,m}, \quad (7.12c)$$

where $\sigma_m = \pm 1$ for $m = 1, \dots, n$ and $M = L, R$.

B. Majorana representation

Since $\widehat{so}(4)_1 = \widehat{su}(2)_1 \oplus \widehat{su}(2)_1$, we can employ four Majorana fields $\hat{\chi}_{M,m}^\mu(x)$ ($\mu = 0, 1, 2, 3$) with $M = L, R$ obeying the equal-time anti-commutators

$$\left\{ \hat{\chi}_{M,m}^\mu(x), \hat{\chi}_{M',m'}^{\mu'}(x') \right\} = \delta_{MM'} \delta_{mm'} \delta_{\mu\mu'} \delta(x-x') \quad (7.13)$$

to describe the $\widehat{su}(2)_1 \oplus \widehat{su}(2)_1$ WZNW model for two decoupled chains making up a single ladder through the Hamiltonian density

$$\hat{H}_{\text{WZNW},m} = \sum_{\mu=0}^3 \frac{i}{2} v \left(\hat{\chi}_{L,m}^\mu \partial_x \hat{\chi}_{L,m}^\mu - \hat{\chi}_{R,m}^\mu \partial_x \hat{\chi}_{R,m}^\mu \right). \quad (7.14)$$

Here, v is the Fermi velocity. Furthermore, the $\widehat{su}(2)_{k=1}$ currents $\hat{J}_{M,m}^a(x)$ and the $\widehat{su}(2)_{k'=1}$ currents $\hat{J}_{M,m}^a(x)$ with

$M = L, R$, $a = 1, 2, 3$, and $m = 1, \dots, n$ can be represented by the bonding linear combination

$$\widehat{\mathcal{K}}_{M,m}^a(x) = \widehat{J}_{M,m}^a(x) + \widehat{J}_{M,m}^a(x) = -\frac{i}{2}\epsilon^{abc}\widehat{\chi}_{M,m}^b(x)\widehat{\chi}_{M,m}^c(x), \quad (7.15a)$$

and the anti-bonding linear combination

$$\widehat{\mathcal{I}}_{M,m}^a(x) = \widehat{J}_{M,m}^a(x) - \widehat{J}_{M,m}^a(x) = -i\widehat{\chi}_{M,m}^0(x)\widehat{\chi}_{M,m}^a(x), \quad (7.15b)$$

respectively. One verifies that $\widehat{\mathcal{K}}_{M,m}^a(x)$ and $\widehat{\mathcal{I}}_{M,m}^a(x)$ generate a closed $\widehat{su}(2)_1 \oplus \widehat{su}(2)_1$ algebra. For later use, we invert Eq. (7.15) to obtain

$$\widehat{J}_{M,m}^a(x) = \frac{1}{2}\left(\widehat{\mathcal{K}}_{M,m}^a(x) + \widehat{\mathcal{I}}_{M,m}^a(x)\right) = \frac{-1}{2}\left(\frac{i}{2}\epsilon^{abc}\widehat{\chi}_{M,m}^b(x)\widehat{\chi}_{M,m}^c(x) + i\widehat{\chi}_{M,m}^0(x)\widehat{\chi}_{M,m}^a(x)\right), \quad (7.16a)$$

$$\widehat{J}_{M,m}^a(x) = \frac{1}{2}\left(\widehat{\mathcal{K}}_{M,m}^a(x) - \widehat{\mathcal{I}}_{M,m}^a(x)\right) = \frac{-1}{2}\left(\frac{i}{2}\epsilon^{abc}\widehat{\chi}_{M,m}^b(x)\widehat{\chi}_{M,m}^c(x) - i\widehat{\chi}_{M,m}^0(x)\widehat{\chi}_{M,m}^a(x)\right). \quad (7.16b)$$

There follows several important consequences from Eq. (7.16).

First, $\widehat{\chi}_{M,m}^0(x)$ transforms under the global diagonal $SU(2)$ symmetry of the WZNW Hamiltonian $\widehat{\mathcal{H}}_{\text{WZNW}}(x)$ as the singlet (trivial) representation, while the triplet $\widehat{\chi}_{M,m}^a(x)$ with $a = 1, 2, 3$ transforms under the same $SU(2)$ as the adjoint representation.

Second, reversal of time that is defined by exchanging left- and right-moving labels together with sign reversal of $\widehat{J}_{M,m}^a(x)$ is represented by complex conjugation in the Fock space spanned by the Majorana fields together with exchanging left- and right-moving labels.

Third, the symmetry under

$$\widehat{J}_{M,m}^a(x) \mapsto \widehat{J}_{M,m}^a(x) \quad \widehat{J}_{M,m}^a(x) \mapsto \widehat{J}_{M,m}^a(x) \quad (7.17)$$

of the WZNW Hamiltonian $\widehat{\mathcal{H}}_{\text{WZNW}}(x)$ is represented by

$$\widehat{\chi}_{M,m}^0(x) \mapsto -\widehat{\chi}_{M,m}^0(x) \quad \widehat{\chi}_{M,m}^a(x) \mapsto +\widehat{\chi}_{M,m}^a(x) \quad (7.18)$$

in the Majorana representation.

Fourth, the relation between the currents and the Majorana fields is one to many since the local gauge transformation

$$\widehat{\chi}_{M,m}^\mu(x) \mapsto \sigma_{M,m}(x)\widehat{\chi}_{M,m}^\mu(x) \quad (7.19)$$

where $\sigma_{M,m}(x) = \pm 1$ leaves the right-hand side of Eq. (7.16) unchanged.

Given the Majorana representation of the $\widehat{su}(2)_1 \oplus \widehat{su}(2)_1$ currents entering the inter-ladder interaction (7.15), we can rewrite the inter-ladder current-current interactions (7.11c) in terms of $4n$ Majorana fields. More specifically, we calculate the inter-ladder interactions (7.11c) by making use of Eq. (7.16). For any $m = 1, \dots, n-1$ and for any $a = 1, 2, 3$, we start from the inter-ladder interaction (7.11c),

$$\left(\widehat{J}_{L,m}^a \widehat{J}_{R,m+1}^a + \widehat{J}_{L,m}^a \widehat{J}_{R,m+1}^a\right) = \frac{1}{2}\left(\widehat{\mathcal{K}}_{L,m}^a \widehat{\mathcal{K}}_{R,m+1}^a + \widehat{\mathcal{I}}_{L,m}^a \widehat{\mathcal{I}}_{R,m+1}^a\right). \quad (7.20)$$

This bilinear form in the currents can be rewritten as a quartic form in terms of the Majorana fields. Thus, the inter-ladder interactions (7.11c) can be written as

$$\widehat{\mathcal{H}}_{\text{inter-ladder},m} = \frac{\lambda}{4}\left[\left(\sum_{a=1}^3 \widehat{\chi}_{L,m}^a \widehat{\chi}_{R,m+1}^a\right)^2 + 2\left(\widehat{\chi}_{L,m}^0 \widehat{\chi}_{R,m+1}^0\right)\left(\sum_{a=1}^3 \widehat{\chi}_{L,m}^a \widehat{\chi}_{R,m+1}^a\right) + \text{const}\right] \quad (7.21a)$$

$$= \frac{\lambda}{4}\left(\sum_{\mu=0}^3 \widehat{\chi}_{L,m}^\mu \widehat{\chi}_{R,m+1}^\mu\right)^2 + \text{const}'. \quad (7.21b)$$

We make three observations.

First, Eq. (7.21a) does not follow if we assume that

the coupling λ breaks the $SU(2)$ symmetry through a

dependence on the index $a = 1, 2, 3$.

Second, Eq. (7.21b) displays an explicit global

$$O(4) = \mathbb{Z}_2 \times SO(4) = \mathbb{Z}_2 \times SO(3) \times SO(3) \quad (7.22)$$

symmetry. This symmetry is broken down to the diagonal subgroup

$$SO(3) \subset SO(4) = SO(3) \times SO(3) \quad (7.23)$$

if Heisenberg interactions between the quantum spin $\widehat{\mathbf{S}}_{i,m}$ and the quantum spin $\widehat{\mathbf{S}}'_{i',m+1}$ are added to the interaction (7.11). Indeed, one verifies that such microscopic perturbations generate $SO(3, 1)$ -symmetric perturbations of the form

$$\left(\sum_{a=1}^3 \chi_{L,m}^a \chi_{R,m+1}^a - \chi_{L,m}^0 \chi_{R,m+1}^0 \right)^2 \quad (7.24)$$

and $SO(3)$ -symmetric perturbations of the form

$$\sum_{a,b,c=1}^3 \epsilon^{abc} \chi_{L,m}^a \chi_{R,m+1}^b \left(\chi_{L,m}^c \chi_{R,m+1}^0 + \chi_{L,m}^0 \chi_{R,m+1}^c \right) \quad (7.25)$$

to the Gross-Neveu-like interaction (7.21b).

Third, the inter-ladder interactions (7.21a) resembles the interactions considered in the paper of Fidkowski and Kitaev³⁰ (see also Ref. 31) in the context of the stability of the topological classification of free fermions when perturbed by interactions.

On the other hand, the intra-ladder interaction (7.11b) is a mere quadratic form when expressed in terms of the Majoranas [c.f. Eq. (6.16)],

$$\widehat{\mathcal{H}}_{\text{intra-ladder},m} = i m_s \widehat{\chi}_{L,m}^0 \widehat{\chi}_{R,m}^0 + \sum_{a=1}^3 i m_t \widehat{\chi}_{L,m}^a \widehat{\chi}_{R,m}^a. \quad (7.26)$$

Here, $m_s, m_t \in \mathbb{R}$ are the bare masses of the Majorana fields.

In short, the lattice model presented in Fig. 2 provides a microscopic realization of the Majorana field theory (2.1) with $v_\mu \equiv v$ for $\mu = 0, 1, 2, 3$, $m_0 \equiv m_s$, and $m_a \equiv m_t$ for $a = 1, 2, 3$. Upon the fine tuning (6.9), (7.5), (7.9),

and $m_s = 0$ from Eq. (6.17a), there only remains three independent couplings out of the seven couplings from the microscopic lattice model. We choose these three independent microscopic couplings to be J_1 , J_\perp , and J_\parallel . They condition the values of the velocity v , triplet mass m_t , and the coupling constant λ for the current-current interaction through

$$v \propto \mathbf{a} J_1, \quad m_t \propto J_\perp, \quad \lambda \propto \mathbf{a} J_\parallel. \quad (7.27)$$

To realize a topologically ordered phase, we need to choose $J_\parallel > 0$, while the signature of J_\perp is arbitrary (see Fig. 3).

To summarize, the Majorana representation of Hamiltonian (7.11) obeying periodic boundary conditions with respect to the coordinates $x \in [0, L_x]$ and $m = 1, \dots, n$ is given by

$$\widehat{\mathcal{H}} = \sum_{m=1}^n \left(\widehat{\mathcal{H}}_{\text{WZNW},m} + \widehat{\mathcal{H}}_{\text{intra-ladder},m} + \widehat{\mathcal{H}}_{\text{inter-ladder},m} \right), \quad (7.28a)$$

$$\widehat{\mathcal{H}}_{\text{WZNW},m} = \sum_{\mu=0}^3 \frac{i}{2} v \left(\widehat{\chi}_{L,m}^\mu \partial_x \widehat{\chi}_{L,m}^\mu - \widehat{\chi}_{R,m}^\mu \partial_x \widehat{\chi}_{R,m}^\mu \right), \quad (7.28b)$$

$$\widehat{\mathcal{H}}_{\text{intra-ladder},m} = i m_s \widehat{\chi}_{L,m}^0 \widehat{\chi}_{R,m}^0 + \sum_{a=1}^3 i m_t \widehat{\chi}_{L,m}^a \widehat{\chi}_{R,m}^a, \quad (7.28c)$$

$$\widehat{\mathcal{H}}_{\text{inter-ladder},m} = \frac{\lambda}{4} \left(\sum_{\mu=0}^3 \widehat{\chi}_{L,m}^\mu \widehat{\chi}_{R,m+1}^\mu \right)^2 + \text{const}' . \quad (7.28d)$$

C. Abelian bosonization

It is instructive to use Abelian bosonization to trade the Majorana representation in Eq. (7.28) for a bosonic one. With the help of the conventions from Secs. VI B and VI C together with some trigonometric identities, one finds

$$\widehat{\mathcal{H}} = \sum_{\mathbf{m}=1}^n \left(\widehat{\mathcal{H}}_{\text{leg},\mathbf{m}}^{\text{upper}} + \widehat{\mathcal{H}}_{\text{leg},\mathbf{m}}^{\text{lower}} + \widehat{\mathcal{H}}_{\text{intra-ladder},\mathbf{m}} + \widehat{\mathcal{H}}_{\text{inter-ladder},\mathbf{m}} \right), \quad (7.29\text{a})$$

$$\widehat{\mathcal{H}}_{\text{leg},\mathbf{m}}^{\text{upper}} = \frac{v}{2} \left[\widehat{\Pi}_{\mathbf{m}}^2 + \left(\partial_x \widehat{\phi}_{\mathbf{m}} \right)^2 \right], \quad \widehat{\mathcal{H}}_{\text{leg},\mathbf{m}}^{\text{lower}} = \frac{v}{2} \left[\widehat{\Pi}_{\mathbf{m}}'^2 + \left(\partial_x \widehat{\phi}'_{\mathbf{m}} \right)^2 \right], \quad (7.29\text{b})$$

$$\widehat{\mathcal{H}}_{\text{intra-ladder},\mathbf{m}} = -\frac{m_t}{\pi \mathbf{a}} \cos \left(\sqrt{2\pi} \left(\widehat{\phi}_{\mathbf{m}} + \widehat{\phi}'_{\mathbf{m}} \right) \right) - \frac{m_t + m_s}{2\pi \mathbf{a}} \cos \left(\sqrt{2\pi} \left(\widehat{\phi}_{\mathbf{m}} - \widehat{\phi}'_{\mathbf{m}} \right) \right) + \frac{m_t - m_s}{2\pi \mathbf{a}} \cos \left(\sqrt{2\pi} \left(\widehat{\theta}_{\mathbf{m}} - \widehat{\theta}'_{\mathbf{m}} \right) \right), \quad (7.29\text{c})$$

$$\widehat{\mathcal{H}}_{\text{inter-ladder},\mathbf{m}} = -\frac{\lambda}{4} \left(\frac{1}{\pi \mathbf{a}} \right)^2 \left[\sum_{\pm} \cos \left(\sqrt{\frac{\pi}{2}} \left[\widehat{\phi}_{\mathbf{m}} + \widehat{\theta}_{\mathbf{m}} + \widehat{\phi}_{\mathbf{m}+1} - \widehat{\theta}_{\mathbf{m}+1} \pm (\text{unprimed} \rightarrow \text{primed}) \right] \right) \right]^2, \quad (7.29\text{d})$$

where it is understood that the trigonometric functions of the bosonic fields must be normal ordered.

The symmetry under the transformation (7.2) becomes the invariance of the bosonic theory defined by Eq. (7.29) under the global transformation

$$\widehat{\theta}_{\mathbf{m}} \mapsto \widehat{\theta}'_{\mathbf{m}}, \quad \widehat{\phi}_{\mathbf{m}} \mapsto \widehat{\phi}'_{\mathbf{m}}, \quad \widehat{\theta}'_{\mathbf{m}} \mapsto \widehat{\theta}_{\mathbf{m}}, \quad \widehat{\phi}'_{\mathbf{m}} \mapsto \widehat{\phi}_{\mathbf{m}}, \quad (7.30)$$

for $\mathbf{m} = 1, \dots, n$.

The symmetry under the transformation (7.3) becomes the invariance of the bosonic theory defined by Eq. (7.29) under the emergent \mathbf{m} -resolved transformation

$$\begin{aligned} \widehat{\phi}_{\mathbf{m}} &\mapsto \widehat{\phi}_{\mathbf{m}} + \sigma_{\mathbf{m}}^{\text{stag}} \sqrt{\frac{\pi}{2}}, & \widehat{\theta}_{\mathbf{m}} &\mapsto \widehat{\theta}_{\mathbf{m}} + \sigma_{\mathbf{m}}^{\text{stag}} \sqrt{\frac{\pi}{2}}, \\ \widehat{\phi}'_{\mathbf{m}} &\mapsto \widehat{\phi}'_{\mathbf{m}} + \sigma_{\mathbf{m}}^{\text{stag}} \sqrt{\frac{\pi}{2}}, & \widehat{\theta}'_{\mathbf{m}} &\mapsto \widehat{\theta}'_{\mathbf{m}} + \sigma_{\mathbf{m}}^{\text{stag}} \sqrt{\frac{\pi}{2}}, \end{aligned} \quad (7.31)$$

where $\sigma_{\mathbf{m}}^{\text{stag}} = 0, 1$ for $\mathbf{m} = 1, \dots, n$, for the arguments of the two cosines on the right-hand side of Eq. (7.29d) change at most by 2π under any one of these transformations.

Evidently, $\widehat{\mathcal{H}}_{\text{intra-ladder},\mathbf{m}}$ and $\widehat{\mathcal{H}}_{\text{intra-ladder},\mathbf{m}+1}$ do not commute with $\widehat{\mathcal{H}}_{\text{inter-ladder},\mathbf{m}}$. Moreover, it is far from obvious that the limit $\lambda = 0$ is nothing but a noninteracting theory of Majorana fields.

However, the bosonic representation (7.29) becomes advantageous in the limit $m_s = m_t = 0$ for which the intra-ladder interaction vanish, as we now explain. In this limit, we are left with the inter-ladder interaction only. The inter-ladder interaction density consists of squaring the sum over two cosines that are given by

$$\cos \left(\sqrt{2\pi} \left(\widehat{\Xi}_{\mathbf{m},\mathbf{m}+1} + \widehat{\Xi}'_{\mathbf{m},\mathbf{m}+1} \right) \right) \quad (7.32\text{a})$$

and

$$\cos \left(\sqrt{2\pi} \left(\widehat{\Xi}_{\mathbf{m},\mathbf{m}+1} - \widehat{\Xi}'_{\mathbf{m},\mathbf{m}+1} \right) \right), \quad (7.32\text{b})$$

respectively, where

$$\widehat{\Xi}_{\mathbf{m},\mathbf{m}+1} := \frac{1}{\sqrt{4}} \left(\widehat{\phi}_{\mathbf{m}} + \widehat{\theta}_{\mathbf{m}} + \widehat{\phi}_{\mathbf{m}+1} - \widehat{\theta}_{\mathbf{m}+1} \right), \quad (7.32\text{c})$$

and

$$\widehat{\Xi}'_{\mathbf{m},\mathbf{m}+1} := \frac{1}{\sqrt{4}} \left(\widehat{\phi}'_{\mathbf{m}} + \widehat{\theta}'_{\mathbf{m}} + \widehat{\phi}'_{\mathbf{m}+1} - \widehat{\theta}'_{\mathbf{m}+1} \right). \quad (7.32\text{d})$$

Now, the linear combination [recall Eq. (6.15)]

$$\widehat{\phi}_{\text{L},\mathbf{m}} := \widehat{\phi}_{\mathbf{m}} + \widehat{\theta}_{\mathbf{m}} \quad \left(\widehat{\phi}'_{\text{L},\mathbf{m}} := \widehat{\phi}'_{\mathbf{m}} + \widehat{\theta}'_{\mathbf{m}} \right) \quad (7.33)$$

defines a left-moving bosonic field on the upper (lower) leg of ladder \mathbf{m} , while the linear combination [recall Eq. (6.15)]

$$\widehat{\phi}_{\text{R},\mathbf{m}+1} := \widehat{\phi}_{\mathbf{m}+1} - \widehat{\theta}_{\mathbf{m}+1} \quad \left(\widehat{\phi}'_{\text{L},\mathbf{m}+1} := \widehat{\phi}'_{\mathbf{m}+1} - \widehat{\theta}'_{\mathbf{m}+1} \right) \quad (7.34)$$

defines a right-moving bosonic field on the upper (lower) leg of ladder $\mathbf{m} + 1$. It follows that, at equal times, $\widehat{\phi}_{\text{L},\mathbf{m}}$ must commute with $\widehat{\phi}_{\text{R},\mathbf{m}+1}$, $\widehat{\phi}'_{\text{L},\mathbf{m}}$ must commute with $\widehat{\phi}'_{\text{R},\mathbf{m}+1}$, $\widehat{\Xi}_{\mathbf{m},\mathbf{m}+1}$ must commute with $\widehat{\Xi}_{\mathbf{m}+1,\mathbf{m}+2}$, $\widehat{\Xi}'_{\mathbf{m},\mathbf{m}+1}$ must commute with $\widehat{\Xi}'_{\mathbf{m}+1,\mathbf{m}+2}$, the cosine (7.32a) must commute with the cosine (7.32b), and

$$\widehat{\mathcal{H}}_{\text{inter-ladder},\mathbf{m}} = -\frac{\lambda}{4} \left(\frac{1}{\pi \mathbf{a}} \right)^2 \left[\cos \left(\sqrt{2\pi} \left(\widehat{\Xi}_{\mathbf{m},\mathbf{m}+1} + \widehat{\Xi}'_{\mathbf{m},\mathbf{m}+1} \right) \right) + \cos \left(\sqrt{2\pi} \left(\widehat{\Xi}_{\mathbf{m},\mathbf{m}+1} - \widehat{\Xi}'_{\mathbf{m},\mathbf{m}+1} \right) \right) \right]^2 \quad (7.35)$$

must commute with $\widehat{\mathcal{H}}_{\text{inter-ladder},\mathbf{m}'}$ for all $\mathbf{m}, \mathbf{m}' = 1, \dots, n$. Hence, the set of operators $\{\widehat{\mathcal{H}}_{\text{inter-ladder},\mathbf{m}}\}$ la-

beled by $\mathbf{m} = 1, \dots, n$ can be simultaneously diagonalized by choosing the eigenfields

$$\Xi_{\mathbf{m},\mathbf{m}+1}(x) \pm \Xi'_{\mathbf{m},\mathbf{m}+1}(x) \quad (7.36a)$$

of

$$\hat{\Xi}_{\mathbf{m},\mathbf{m}+1}(x) \pm \hat{\Xi}'_{\mathbf{m},\mathbf{m}+1}(x) \quad (7.36b)$$

to be either

$$\Xi_{\mathbf{m},\mathbf{m}+1}(x) \pm \Xi'_{\mathbf{m},\mathbf{m}+1}(x) = 0 + \sqrt{2\pi} n_{\mathbf{m},\mathbf{m}+1}^{\pm}, \quad n_{\mathbf{m},\mathbf{m}+1}^{\pm} \in \mathbb{Z}, \quad (7.36c)$$

or

$$\Xi_{\mathbf{m},\mathbf{m}+1}(x) \pm \Xi'_{\mathbf{m},\mathbf{m}+1}(x) = \sqrt{\frac{\pi}{2}} + \sqrt{2\pi} n_{\mathbf{m},\mathbf{m}+1}^{\pm}, \quad n_{\mathbf{m},\mathbf{m}+1}^{\pm} \in \mathbb{Z}. \quad (7.36d)$$

Any eigenvalue from the family (7.36c) is to be interpreted as the positive expectation value

$$\left\langle \text{GS}; + \left| \sum_{\mu=0}^3 i\hat{\chi}_{L,\mathbf{m}}^{\mu} \hat{\chi}_{R,\mathbf{m}+1}^{\mu} \right| \text{GS}; + \right\rangle \equiv +C > 0 \quad (7.37a)$$

in the ground state $|\text{GS}; +\rangle$. Any eigenvalue from the family (7.36d) is to be interpreted as the negative expectation value

$$\left\langle \text{GS}; - \left| \sum_{\mu=0}^3 i\hat{\chi}_{L,\mathbf{m}}^{\mu} \hat{\chi}_{R,\mathbf{m}+1}^{\mu} \right| \text{GS}; - \right\rangle \equiv -C < 0 \quad (7.37b)$$

in the ground state $|\text{GS}; -\rangle$. Any non-vanishing value of $C > 0$ breaks spontaneously the M- and \mathbf{m} -resolved symmetry under the transformation (2.6) of Hamiltonian (7.28) in the limit $m_s = m_t = 0$ [any non-vanishing value of $C > 0$ also breaks spontaneously the \mathbf{m} -resolved symmetry under the transformation (2.3) of Hamiltonian (7.28) for any one of m_s or m_t non-vanishing].

Classical static \mathbf{m} -resolved solitons are time-independent eigenfields (7.36a) that (i) interpolate between any pair from the classical minima enumerated in Eqs. (7.36c) and (7.36d) as x interpolates from $x = -\infty$ to $x = +\infty$ (ii) and whose energy density is of compact support with respect to $x \in \mathbb{R}$.

Following Refs. 20 and 32, we identify among all such solitons four types of \mathbf{m} -resolved elementary solitons. A type-I \mathbf{m} -resolved soliton corresponds to both $\Xi_{\mathbf{m},\mathbf{m}+1} + \Xi'_{\mathbf{m},\mathbf{m}+1}$ and $\Xi_{\mathbf{m},\mathbf{m}+1} - \Xi'_{\mathbf{m},\mathbf{m}+1}$ increasing monotonically in their values by the amount $\sqrt{\pi/2}$ between $x = -\infty$ to $x = +\infty$. A type-II \mathbf{m} -resolved soliton corresponds to both $\Xi_{\mathbf{m},\mathbf{m}+1} + \Xi'_{\mathbf{m},\mathbf{m}+1}$ and $\Xi_{\mathbf{m},\mathbf{m}+1} - \Xi'_{\mathbf{m},\mathbf{m}+1}$ decreasing monotonically in their values by the amount $\sqrt{\pi/2}$ between $x = -\infty$ to $x = +\infty$. A type-III \mathbf{m} -resolved

soliton can be thought of as an \mathbf{m} -resolved anti-soliton of type I. A type-III \mathbf{m} -resolved soliton corresponds to $\Xi_{\mathbf{m},\mathbf{m}+1} + \Xi'_{\mathbf{m},\mathbf{m}+1}$ ($\Xi_{\mathbf{m},\mathbf{m}+1} - \Xi'_{\mathbf{m},\mathbf{m}+1}$) increasing (decreasing) monotonically in value by the amount $\sqrt{\pi/2}$ between $x = -\infty$ to $x = +\infty$. A type-IV soliton corresponds to $\Xi_{\mathbf{m},\mathbf{m}+1} + \Xi'_{\mathbf{m},\mathbf{m}+1}$ ($\Xi_{\mathbf{m},\mathbf{m}+1} - \Xi'_{\mathbf{m},\mathbf{m}+1}$) decreasing (increasing) monotonically in values by the amount $\sqrt{\pi/2}$ between $x = -\infty$ to $x = +\infty$. A type-IV \mathbf{m} -resolved soliton can be thought of as and \mathbf{m} -resolved anti-soliton of type III. Upon quantization, Witten has shown in Ref. 20 that we may associate these four types of elementary solitons to point-like many-body excitations that form a four-dimensional irreducible representation of a Clifford algebra with four generators.

Solitons of type I, II, III, and IV interpolate between any pair with one classical minima from the family (7.36c) and the other classical minima from the family (7.36d) as x interpolates from $x = -\infty$ to $x = +\infty$. Such solitons should be distinguished from those solitons that interpolate between any pair with both classical minima from either one of the two families (7.36c) and (7.36d) as x interpolates from $x = -\infty$ to $x = +\infty$. The former solitons are associated with the spontaneous breaking of the chiral symmetry. The solitons associated with two classical minima of either one of the families (7.36c) or (7.36d) differing by $\delta n_{\mathbf{m},\mathbf{m}+1}^{\pm} = \pm 1$ while $\delta n_{\mathbf{m},\mathbf{m}+1}^{-} = 0$ are associated with the spontaneous breaking of the symmetry (7.31).

We close this discussion by deriving the sine-Gordon representation (4.4) of Hamiltonian (7.29) in the limit of vanishing intra-ladder interaction. The sine-Gordon Hamiltonian (4.4) follows from expanding the squared bracket on the right-hand side of Eq. (7.35). There are four products of normal-ordered cosine interactions in this expansion. Two of them involve squaring the same normal-ordered cosine operator. This exercise requires combining point splitting with the operator product expansion and results in a renormalization of the kinetic contributions (7.29b). The remaining two products of normal-ordered cosine interactions involve distinct commuting operators for which we can use the decomposition rule for the multiplication of two cosines into the addition of two cosines. The sine-Gordon Hamiltonian (4.4) follows with the identifications

$$\hat{\varphi}_s := \frac{\sqrt{8\pi}}{\beta} \hat{\Xi}_{\mathbf{m},\mathbf{m}+1}, \quad \hat{\varphi}_c := \frac{\sqrt{8\pi}}{\beta} \hat{\Xi}'_{\mathbf{m},\mathbf{m}+1}. \quad (7.38a)$$

D. Spontaneous symmetry breaking

We have shown that Hamiltonian (7.29) commutes with any one of the $2n+1$ transformations

$$\widehat{\phi}_m \mapsto \widehat{\phi}_m + 2\sigma_m \sqrt{\frac{\pi}{2}}, \quad \widehat{\theta}_m \mapsto \widehat{\theta}_m, \quad \widehat{\phi}'_m \mapsto \widehat{\phi}'_m, \quad \widehat{\theta}'_m \mapsto \widehat{\theta}'_m, \quad \text{Majorana redundancy} \quad (7.39a)$$

$$\widehat{\phi}_m \mapsto \widehat{\phi}'_m, \quad \widehat{\theta}_m \mapsto \widehat{\theta}'_m, \quad \widehat{\phi}'_m \mapsto \widehat{\phi}_m, \quad \widehat{\theta}'_m \mapsto \widehat{\theta}_m, \quad \widehat{S}_{i,m} \leftrightarrow \widehat{S}'_{i,m} \quad (7.39b)$$

$$\widehat{\phi}_m \mapsto \widehat{\phi}_m + \sigma_m \sqrt{\frac{\pi}{2}}, \quad \widehat{\theta}_m \mapsto \widehat{\theta}_m + \sigma_m \sqrt{\frac{\pi}{2}}, \quad \widehat{\phi}'_m \mapsto \widehat{\phi}'_m + \sigma_m \sqrt{\frac{\pi}{2}}, \quad \widehat{\theta}'_m \mapsto \widehat{\theta}'_m + \sigma_m \sqrt{\frac{\pi}{2}}, \quad \widehat{S}_{i,m}^{(\prime)} \mapsto \widehat{S}_{i+1,m}^{(\prime)} \quad (7.39c)$$

with $\sigma_m = 0, 1$ for $m = 1, \dots, n$.

All these transformations commute pairwise and their action on the trigonometric functions entering Hamiltonian (7.29) is involutive. Consequently, all many-body energy eigenstates of Hamiltonian (7.29) are 2^{2n} -fold degenerate with the decomposition

$$2^{2n} = 2^{n-1} \times 2 \times 2^n, \quad (7.40)$$

whereby the factor 2^{n-1} arises from the Majorana redundancy as was deduced after Eq. (5.13), the factor 2 arises from the global symmetry under the exchange of unprimed and primed fields in all ladders, and the factor 2^n arises from the reversal in sign of all the staggered fields in an arbitrarily chosen ladder. The degeneracy 2^{n-1} was shown to be broken spontaneously at and only at zero temperature through the breaking of the chiral symmetry encoded by the order parameter (2.7) in the Majorana representation. The remaining degeneracy 2×2^n remains unbroken all the way to and at zero temperature, as is evident from the fact that the chiral order parameter for the Majorana fermions is invariant under the transformations (7.39b) and (7.39c). In particular, the degeneracy 2^n is invisible to the Majorana fields. Hence, the topological degeneracy in the phase diagram from Fig. 3 coexists with the 2^{2n} degeneracy associated with the symmetries (7.39a), (7.39b), and (7.39c). Whereas the degeneracy 2^{n-1} associated to the symmetry (7.39a) originates from the redundancy of the m -resolved Majorana representation of the conserved chiral currents (7.15) and, as such, is intrinsic to the Majorana representation and invisible to any probe from the Fock space generated by the spin-1/2, the degeneracy 2×2^n associated with the symmetries (7.39b) and (7.39c) is specific to any microscopic Hamiltonian with the global symmetry (7.2) and a ladder-resolved extension of the global symmetry (7.3). In other words, the degeneracy 2^n resulting from the m -resolved symmetry under the transformation (7.39c) is not intrinsic to the microscopic inter-ladder interaction (7.1), but emerges from neglecting perturbations to the inter-ladder Hamiltonian (7.11c) [see also Eqs. (7.28d) or (7.29d)] that we now discuss.

E. Competing instabilities

The ATO and NATO phases of the effective low-energy theory encoded by Hamiltonian (2.1) compete with the ordered phases that are stabilized by the longer-range interaction densities of the forms

$$[\widehat{n}_m(x) + \sigma \widehat{n}'_m(x)] \cdot [\widehat{n}_{m+r}(x) + \sigma' \widehat{n}'_{m+r}(x)], \quad (7.41a)$$

$$[\widehat{\varepsilon}_m(x) + \sigma \widehat{\varepsilon}'_m(x)] [\widehat{\varepsilon}_{m+r}(x) + \sigma' \widehat{\varepsilon}'_{m+r}(x)], \quad (7.41b)$$

$$[\widehat{n}_m(x) + \sigma \widehat{n}'_m(x)] \cdot \partial_x [\widehat{n}_{m+r}(x) + \sigma' \widehat{n}'_{m+r}(x)], \quad (7.41c)$$

$$[\widehat{\varepsilon}_m(x) + \sigma \widehat{\varepsilon}'_m(x)] \cdot \partial_x [\widehat{\varepsilon}_{m+r}(x) + \sigma' \widehat{\varepsilon}'_{m+r}(x)], \quad (7.41d)$$

where $\sigma, \sigma' = \pm 1$ and $|r| > 1$. (Here we recall that, by design, all the bare couplings vanish for $r = 1$.)

One consequence of these interaction densities is that they can remove the emergent m -resolved symmetry under the transformation (7.12) [(7.39c)]. The fate (confinement versus deconfinement) of the solitons associated with the spontaneous breaking of the symmetry (7.12) [(7.39c)] in the presence of such symmetry-breaking interactions is left for future work.

The perturbative renormalization group allows to assess the potency of the competing interaction densities (7.41) relative to the inter-ladder interaction density (7.11c) [see also Eqs. (7.28d) or (7.29d)].

On the one hand, the interactions densities (7.41c) and (7.41d) are marginal perturbations of the critical theory (7.28b). As such, they can be safely ignored provided their coupling constants are smaller than the couplings of the leading current-current interactions.

On the other hand, the interaction densities (7.41a) and (7.41b) are relevant perturbations of the critical theory (7.28b). As such, they present certain difficulties. For the spin-1/2 lattice Hamiltonian that we have chosen, their coupling constants are of the order of $\sim J_V^2/J_1$, but cannot be reliably determined otherwise. The problem is that at small microscopic bare couplings $\chi \ll J_1$ and $J_V \ll J_1$, the spectral gap M of the effectively one-dimensional Hamiltonian (2.5) that originates from the marginal current-current interaction is exponentially small in the effective coupling λ of Hamiltonian (2.5). Hence, to make M larger than $\sim J_V^2/J_1$, we have to go in the region of intermediate to strong bare couplings λ/J_1 ,

with λ defined in Eq. (7.6b). Our methods do not allow to establish whether the required parameter regime exists or whether it can be reached for some modification of the lattice Hamiltonian. We take heart from the fact that the required regime of large energy gap $M \sim J_1$ exists in the frustrated quantum spin 1/2 zig-zag ladder with a three-spin interaction that was studied by Frahm and Rödenbeck in Ref. 33. They demonstrated that, under certain conditions corresponding to our $\lambda = 0$ in Eq. (7.11c), their ladder is integrable with a spectrum that is partially gapped with a gap of order of the leading exchange interaction, J_1 in our setting. In this case, the mass M exceeds the energy scale for the characteristic energy scales associated to the relevant interactions from Eq. (7.41), in which case their neglect in the effective Hamiltonian (2.1) would be a posteriori consistent. Ultimately, however, only numerical calculations can establish that the Majorana field theory (2.1) captures the low energy physics of the microscopic spin 1/2 lattice model.

VIII. SUMMARY

In this paper, we put an emphasis on finding a field theory which would lead to non-Abelian topological order. We used the methods of quantum-field theory to solve a fermionic model with a topologically nontrivial ground state. We also presented a candidate lattice spin model whose low energy sector is described by this fermionic theory, namely, a model of quantum spin $S = 1/2$ ladders coupled by a three-spin interaction. We found that the bulk spectrum of the fermionic model is gapped and that there are robust chiral gapless modes on the boundaries. There are two topologically nontrivial phases. In one of them the boundary modes are described by a single species of gapless Majorana fermions. This phase realizes a Nonabelian Topological Order (NATO). In the

other phase, the boundary modes are four gapless modes. This phase realizes an Abelian Topological Order (ATO). In both cases the bulk excitations are gapped. We found that their spectrum consists of two types of particles. Particles of one type are Majoranas. They propagate in two-dimensional space. Particles of the other type are fractionalized solitons which remain confined to individual ladders. Since the Majoranas are bound states of these particles, their spectrum is situated below the soliton-antisoliton continuum.

Since spin operators are bosonic, single Majoranas cannot be observed by measuring spin-spin correlation functions. However, their presence can be ascertained by measurements of thermal transport which are sensitive to their statistics.

The presence of the solitons is a sign of the extensive ground-state degeneracy in the fermionic sector of the theory. This degeneracy is associated with the existence of an order parameter that is not local in the original spin variables. Hence, any operator that is local in the spins has no access to this degeneracy.

ACKNOWLEDGMENTS

J.-H. C. was supported by the Swiss national Science Foundation (SNSF) under Grant No. 2000021 153648. C. C. was supported by the U.S. Department of Energy (DOE), Division of Condensed Matter Physics and Materials Science, under Contract No. DE-FG02-06ER46316. A. M. T. was supported by the U.S. Department of Energy (DOE), Division of Condensed Matter Physics and Materials Science, under Contract No. DE-AC02-98CH10886. We acknowledge the Condensed Matter Theory Visitors Program at Boston University for support. A. M. T. is grateful to Alexander Abanov for valuable discussions. We thank Yohei Fuji for constructive criticisms.

-
- ¹ X.-G. Wen, *Int. J. Mod. Phys. B* **05**, 1641 (1991).
² A. Kitaev and J. Preskill, *Phys. Rev. Lett.* **96**, 110404 (2006).
³ M. Levin and X.-G. Wen, *Phys. Rev. Lett.* **96**, 110405 (2006).
⁴ X. Chen, Z.-C. Gu, and X.-G. Wen, *Phys. Rev. B* **82**, 155138 (2010).
⁵ X.-G. Wen, *Nat. Sci. Rev.* **3**, 68 (2016).
⁶ T. Lan, L. Kong, and X.-G. Wen, *Phys. Rev. B* **94**, 155113 (2016).
⁷ R. Moessner and S. L. Sondhi, *Phys. Rev. Lett.* **86**, 1881 (2001).
⁸ A. Kitaev, *Annals of Physics* **321**, 2 (2006).
⁹ R. Mukhopadhyay, C. L. Kane, and T. C. Lubensky, *Phys. Rev. B* **63**, 081103 (2001).
¹⁰ C. L. Kane, R. Mukhopadhyay, and T. C. Lubensky, *Phys. Rev. Lett.* **88**, 036401 (2002).
¹¹ J. C. Y. Teo and C. L. Kane, *Phys. Rev. B* **89**, 085101 (2014).
¹² C. L. Kane, A. Stern, and B. I. Halperin, *Phys. Rev. X* **7**, 031009 (2017).
¹³ S. Chakravarty, *Phys. Rev. Lett.* **77**, 4446 (1996).
¹⁴ G. Sierra, *J. Phys. A: Math. Gen.* **29**, 3299 (1996).
¹⁵ G. Sierra, “On the application of the non-linear sigma model to spin chains and spin ladders,” in *Strongly Correlated Magnetic and Superconducting Systems: Proceedings of the El Escorial Summer School Held in Madrid, Spain, 15–19 July 1996*, edited by G. Sierra and M. A. Martín-Delgado (Springer Berlin Heidelberg, Berlin, Heidelberg, 1997) pp. 137–166.
¹⁶ O. F. Syljuåsen, S. Chakravarty, and M. Greven, *Phys. Rev. Lett.* **78**, 4115 (1997).
¹⁷ T. Neupert, C. Chamon, C. Mudry, and R. Thomale, *Phys. Rev. B* **90**, 205101 (2014).
¹⁸ P.-H. Huang, J.-H. Chen, P. R. S. Gomes, T. Neupert, C. Chamon, and C. Mudry, *Phys. Rev. B* **93**, 205123 (2016).

- ¹⁹ P.-H. Huang, J.-H. Chen, A. E. Feiguin, C. Chamon, and C. Mudry, *Phys. Rev. B* **95**, 144413 (2017).
- ²⁰ E. Witten, *Nuclear Physics B* **142**, 285 (1978).
- ²¹ S. Lukyanov and A. Zamolodchikov, *Nuclear Physics B* **607**, 437 (2001).
- ²² F. H. L. Essler and A. M. Tsvelik, *Phys. Rev. B* **65**, 115117 (2002).
- ²³ F. H. L. Essler and A. M. Tsvelik, *Phys. Rev. B* **71**, 195116 (2005).
- ²⁴ D. G. Shelton, A. A. Nersesyan, and A. M. Tsvelik, *Phys. Rev. B* **53**, 8521 (1996).
- ²⁵ A. A. Nersesyan and A. M. Tsvelik, *Phys. Rev. Lett.* **78**, 3939 (1997).
- ²⁶ A. O. Gogolin, A. A. Nersesyan, and A. M. Tsvelik, *Bosonization and Strongly Correlated Systems* (Cambridge University Press, 2004).
- ²⁷ A. M. Tsvelik, *Quantum Field Theory in Condensed Matter Physics* (Cambridge University Press, 2003).
- ²⁸ D. Allen, F. H. L. Essler, and A. A. Nersesyan, *Phys. Rev. B* **61**, 8871 (2000).
- ²⁹ G. Gorohovsky, R. G. Pereira, and E. Sela, *Phys. Rev. B* **91**, 245139 (2015).
- ³⁰ L. Fidkowski and A. Kitaev, *Phys. Rev. B* **81**, 134509 (2010).
- ³¹ H. Yao and S. Ryu, *Phys. Rev. B* **88**, 064507 (2013).
- ³² R. Shankar and E. Witten, *Nuclear Physics B* **141**, 349 (1978).
- ³³ H. Frahm and C. Rdenbeck, *Journal of Physics A: Mathematical and General* **30**, 4467 (1997).